AWARD NUMBER: **W81XWH-14-1-0465**

TITLE: **Early Intervention Stem Cell-Based Therapy (EISCBT) for Corneal Burns and Trauma**

PRINCIPAL INVESTIGATOR: **James L Funderburgh**

CONTRACTING ORGANIZATION:

**The University of Pittsburgh
Pittsburgh PA 15213**

REPORT DATE: **October 2016**

TYPE OF REPORT: **Annual**

PREPARED FOR: U.S. Army Medical Research and Materiel Command
Fort Detrick, Maryland, 21702-5012

DISTRIBUTION STATEMENT: Approved for Public Release;
Distribution Unlimited

The views, opinions and/or findings contained in this report are those of the author(s) and should not be construed as an official Department of the Army position, policy or decision unless so designated by other documentation.

REPORT DOCUMENTATION PAGE		*Form Approved*

Public reporting burden for this collection of information is estimated to average 1 hour per response, including the time for reviewing instructions, searching existing data sources, gathering and maintaining the data needed, and completing and reviewing this collection of information. Send comments regarding this burden estimate or any other aspect of this collection of information, including suggestions for reducing this burden to

1. REPORT DATE October 2016	2. REPORT TYPE: Annual	3. DATES COVERED 22 Sept 2015 - 21 Sept 2016
4. TITLE AND SUBTITLE Early Intervention Stem Cell-Based Therapy (EISCBT) for Corneal Burns and Trauma		**5a. CONTRACT NUMBER** W81WH-14-1-0465
		5b. GRANT NUMBER
		5c. PROGRAM ELEMENT NUMBER
6. AUTHOR(S) James L Funderburgh **E-Mail**: jlfunder@pitt.edu		**5d. PROJECT NUMBER**
		5e. TASK NUMBER
		5f. WORK UNIT NUMBER
7. PERFORMING ORGANIZATION NAME(S) AND ADDRESS(ES) University of Pittsburgh Office of Research 123 University Place, B21 Pittsburgh , PA 15213-2303		**8. PERFORMING ORGANIZATION REPORT NUMBER**
9. SPONSORING / MONITORING AGENCY NAME(S) AND ADDRESS(ES) U.S. Army Medical Research and Materiel Command Fort Detrick, Maryland 21702-5012		**10.SPONSOR/MONITOR'S ACRONYM(S)**
		11. SPONSOR/MONITOR'S REPORT NUMBER(S)

12. DISTRIBUTION / AVAILABILITY STATEMENT
Approved for Public Release; Distribution Unlimited

13. SUPPLEMENTARY NOTES

14. ABSTRACT

The goal of this project is to develop a stem cell-based regenerative corneal bandage (ReCoBand) that can be applied in the battlefield to prevent permanent scarring of the cornea after trauma, blast, or burn wounds. In the second year of this project we have: (1) developed an assay to characterized anti-inflammatory properties of human corneal stem cells, (2) used the assay to compare cell lines isolated from 20 different individual donors, (3) carried out RNAseq on six cell lines with high and low anti-inflammatory properties and used bioinformatics on the RNAseq data to discover a set of marker genes that can be used to screen cell lines for anti-inflammatory properties. Additionally we have (4) developed a wound healing assay in mice to measure the extent to which stem cells block corneal scarring, (5) carried out preliminary experiments demonstrating that stem cells in plastic-compressed collagen gels are highly effective at preventing scarring when applied to the surface of a wounded eye, and (6) showed that that the gel-embedded stem cells can be cryopreserved. These accomplishments meet the proposed milestones and predict success in meeting the overall goals of the project by the end of its 3 year time-course.

15. SUBJECT TERMS
cornea, scarring, stem cells, regeneration, plastic-compressed collagen, anti-inflammatory, RNAseq, gene expression.

16. SECURITY CLASSIFICATION OF:			17. LIMITATION OF ABSTRACT	18. NUMBER OF PAGES	19a. NAME OF RESPONSIBLE PERSON USAMRMC
a. REPORT Unclassified	**b. ABSTRACT** `Unclassified`	**c. THIS PAGE** Unclassified	Unclassified	92	**19b. TELEPHONE NUMBER** *(include area code)*

Table of Contents

1. INTRODUCTION:

Corneal trauma and chemical burns lead to corneal scarring, producing a long-term reduction in vision, sometimes blindness. Corneal scarring and decompensation are the second-most common causes of poor vision among ocular injuries in combat, commonly caused by explosions with fragmentary munitions and by chemical and thermal exposure. This project will develop a therapeutic device (ReCoBand) containing live stem cells that can be applied to the cornea, in a field hospital to eyes with trauma or burns to prevent long-term scarring or blindness. The first aim of this project was to identify genes in corneal stromal stem cells (CSSC) that correlate with their ability to block scarring. The second phase of the project is focused on development of a system deliver the CSSC to the cornea to act as a regenerative corneal bandage (ReCoBand). These bandages can be held in place on the cornea by a soft contact lens. In the third phase of the project we will optimize means of storing the ReCoBand frozen so they will be available to doctors in field hospitals. Additionally we will investigate the timing for the start of therapy to determine how soon does the bandage need to be put in place after an injury. The type and severity of the injury that can be treated will also be addressed. At the end of the three-year project we will have defined the components required to create a novel treatment system that prevents corneal scarring that can move directly into an application to the FDA for a new 'biologic device'. Because the stem cells in this device do not actually enter the body, this device will be considered safer than procedures involving transplantation of stem cell and thus may move to clinical trials in a timely manner. If successful, the ReCoBand may save vision of many and reduce the need for corneal transplantation.

2. KEYWORDS: Vision, Blindness, Cornea, Scarring, Stem Cells, Cell based therapy, inflammation, immunomodulation

3. ACCOMPLISHMENTS:

Major goals and objectives of the project:

- Develop a metric for analysis of stem cell regenerative potential
- Demonstrate the roles of specific genes in stromal regeneration in vivo
- Assess plastic compressed collagen as a stem cell delivery vehicle
- Assess cell sheets as delivery vehicle for stem cells.
- Determine type of injury and timing for which corneal stem cell-based therapy is most effective.

Milestones:
1. Milestone (12 months): Isolation of a library of CSSC lines with identified gene expression phenotypes. **Achieved**
2. Milestone (24 months): Identification of stem cell genes required for suppression of scarring in vivo. **Achieved**
3. Milestone (24 months): Assessment of plastic compressed collagen as stem cell delivery vehicle. **Achieved**
4. Milestone (30 months) : Assessment of cell sheets as stem cell delivery vehicle. Milestone(s) (36 months): Understanding the time frame and injury type for which stem cell therapy will be useful vehicle.

What was accomplished under these goals?

Corneal Stromal Stem Cells (CSSC) are obtained from biopsies of corneal tissue. The quality and potency of individual stem cell lines varies greatly from one individual to another. A major hurdle for developing a standardized stem cell therapeutic reagent is determining potency of the cells. Our approach to determining this was collection of a library of 24 cell lines from different individual donors and comparison of them as to their gene expression, and biological properties. The goal is to define a set of genes that allow rapid screening of any cell line to determine its potential for therapeutic use in treating corneal damage. In the first year of the project we collected tissue, derived cell lines and compared assays for their ability to exert anti-inflammatory properties.

Activities, objectives, results *for year-two of this project are summarized for seven different aims proposed in the original grant. These are illustrated with figures in Appendix 1. Discussion of additional findings is included under the heading of "Other Achievements."*

(1) Aim 1B Subtask 3. We developed an assay to characterized anti-inflammatory properties of human corneal stem cells. In the original grant we proposed the use of mouse macrophages to test the anti-inflammatory properties of stem cells. We have modified that methodology to use a mouse macrophage cell line (RAW 264.7) which is more repeatable and may be more suitable for a standardized SOP in an approved clinical trial. The RAW cells are subject to conditions that upregulate several specific differentiation-related genes in response to stimulation with a peptide RANKL (**R**eceptor **A**ctivating **N**F **K**appa-B **L**igand). This response involves activation of NF-Kappa B, an essential signaling system mediating most inflammatory responses. Activation of RAW cell differentiation has been extensively used to assess the effectiveness of anti-inflammatory materials. In our case we found that the response to RANKL was reduced in a concentration dependent manner by conditioned culture media from CSSC cells. (Fig 1, Appendix 1).

(2) Aim 1B Subtask 3. We used the assay to compare cell lines isolated from 20 different individual donors. Conditioned media from the different lines were used to inhibit differentiation of RAW cells as in Figure 1. There was a distinct difference among lines that was repeatable. The average expression of three genes was combined to obtain assessment of the most strongly anti-inflammatory (AIF-High) CSSC versus the least anti-inflammatory (AIF-Low) cells. (Fig 2 Appendix 1)

(3) Aim 1A Subtask 2. Six cell lines (3 AIF-High and 3 AIF-Low) (Fig 2) were selected for RNAseq analysis. Bioinformatics cluster analysis of the results demonstrated that the IS-H and IS-L had distinct phenotypes in terms of their gene expression pattern (Fig 3A, Appendix 1). Expression analysis was used to identify a set of genes that can be used as markers of the immunosuppressive phenotype (Fig 3B, Appendix 1). The list of marker genes differs from those identified previously as "stem cell markers" and thus can provide a unique tool for selecting cells effective at suppressing inflammation and inducing regeneration of native tissue. This list is shown in Table 1 (Appendix 1).

(4) Aim 1B Subtask 5. We have adapted our wound healing assay to screen CSSC cell lines to measure the extent to which stem cells block corneal scarring. Stromal tissue is ablated using an Algerbrush II (under full anesthesia). Scarring is imaged in the whole eye at 2-weeks using indirect lighting. Intensity of scarring is quantified using scar area determined by image analysis of wounded eyes. qPCR of corneal RNA from wounded corneas

(5) Aim 2A Subtask Carried out preliminary experiments demonstrating that stem cells in plastic-compressed collagen gels are highly effective at preventing scarring when applied to the surface of a wounded eye Fig 4, (Appendix 1). The gels adhered to the mouse cornea and were in place for 24 hr. By 48 hr both gels and stem cells were no longer present on the ocular surface. We attribute this to the high level of collagenase and other metalloproteinases secreted by the CSSC (data not shown). In spite of the short duration of the gel on the ocular surface, gels containing CSSC effectively suppressed scar formation lending credence to our hypothesis regarding the utility of the ReCoBand.

(5) Aim 2B Subtask 4. Showed that that the gel-embedded stem cells can be cryopreserved. Gels equilibrated with conventional cryopreservation media were found to contain a high proportion of viable cells after thawing Fig 5, (Appendix 1). This again adds to our confidence that the ReCoBand device will function as proposed.

Other Achievements. We observed that small membrane microvesicles (exosomes) isolated from CSSC-conditioned media were able to suppress RAW cell differentiation Fig 6C (Appendix 1) and to prevent scarring in our murine wound healing model Fig 6D. CSSC exosomes have the advantage that as non-viable material they will be easier to gain regulatory approval for human use. Importantly, these vesicles are much more likely to be stable in storage conditions that could allow them to be transported forward in a battlefield situation without the need ultralow temperature cryopreservation, thus making them more effective for treatment of wounded warriors. Grants Officer, Elena Howell and Research Analyst/ Science Officer, Marc L. Mitchell have provided opinions by email that pursuing the potential use of CSSC-derived exosomes is within the scope and original SOW of this project.

What opportunities for training and professional development has the project provided?

Dr. Syed-Picard who served for 8 months on this project as a research associate and obtained valuable skills in cell techniques. Based on some of the work funded by this project Dr. Syed-Picard has been awarded a NIH K99/R00 and has accepted an Assistant Professor position in the Department of Dentistry. She is listed as first Author on a submitted manuscript (Appendix 3).

Dr. Golnar Shoshaati has served in the postdoctoral position of this project since September 2015 and will be leaving to set up a research lab in Zurich Switzerland, her home country. Dr. Shoshaati had no formal research training before joining this project but has become a fully competent cornea researcher. She is listed a co-first author on a recently submitted paper (Appendix 4). The program has trained her in translational corneal research which she expects to continue as an independent researcher in Switzerland. We hope to continue a collaboration in the next phase of the project, perhaps in developing initial clinical trials.

A new Postdoctoral Associate has joined the project. Dr. Irona Khandaker is a specialist in Bioinformatics and is learning the techniques of regenerative biology in this project. We expect, like her predecessors, Dr. Khandaker will move into a professional research position at the end of this project.

How were the results disseminated to communities of interest?

Two manuscripts describing some of the data developed in the first two years of the project have been submitted for publication. These are attached as Appendix 3 and 4. The publication announcements will be forwarded to the DoD on receipt. The results of the supported research were also presented at several meetings including Association for Research in Vision and Ophthalmology (ARVO), Seattle May 2016. Abstracts of these presentations are attached Appendix 6 and 5.

What do you plan to do during the next reporting period to accomplish the goals?

Several important goals remain in the project:

- How do the anti-inflammatory marker genes identified by RNAseq/qPCR correlate with ability of a cell line to suppress scarring and regenerate native corneal tissue.

- What is the crucial window of timing for application of the ReCoBand after injury.

- Can the cryopreserved ReCoBand gels suppress corneal scarring ?

- Can CSSC in a different format; e.g. scaffold-free cell sheets (see Manuscript (Appendix 3) compare with the gel-based ReCoBand in terms of corneal regenerative abilities.

- How does the healing of traumatic wounds compare with that corneal chemical burns.

- In addition to those **approved** from the original application, we will continue to investigate the effectiveness of CSSC based exosomes, because of their high translation potential. Grants officer, Elena Howell and Research Analyst/ Science Officer, Marc L. Mitchell have provided opinions by email that pursuing the potential use of CSSC derived exosomes is within the scope and original SOW of this project.

4. IMPACT:

What was the impact on the development of the principal discipline(s) of the project?

Work with adult stem cells focuses largely on the potential of these cells. Cells are often used without purification and characterized by expression of a set of cell surface proteins found on many mesenchymal cells. Little effort has gone into understanding how potent a particular line of cells is, and if cells from different individuals vary. Our work is on track to illustrate an important fact that stem cells vary markedly in their potential according to their source and that defining criteria for assessing that potency will be essential for translating their use to the clinic.

What was the impact on other disciplines? Nothing to Report

What was the impact on technology transfer? Nothing to Report

What was the impact on society beyond science and technology? Nothing to Report

5 CHANGES/PROBLEMS:

Changes in approach and reasons for change.

We observed (Fig 1) that conditioned culture media from CSSC had an anti-inflammatory effect similar to co-culture with cells. We have since observed that microvesicles present in conditioned media can duplicate the effect, both in suppression of RAW cell differentiation Because of the clear advantages of a stable non-living material in the ReCoBand (discussed above) , we will continue to investigate the potential use of exosomes.

Actual or anticipated problems or delays and actions or plans to resolve them.

The initial delay in defining cell lines with high regenerative potential pushed back the RNAseq analysis of these lines by 1-2 months. This analysis was originally planned for CY15Q4, but was delayed CY16Q3. This change did not impact the overall time course of the project.

Changes that have a significant impact on expenditures. Nothing to Report

Significant changes in use or care of human subjects, vertebrate animals, biohazards, and/or select agents. Nothing to Report

6. PRODUCTS

Publications, conference papers, and presentations
- Oral Presentation at ARVO (Association for Research in Vision and Ophthalmology)Seattle May , 2016Abstracts in Appendix
- Two manuscripts citing DoD support have been submitted for publication. Copies are in Appendix.

Technologies or techniques- Nothing to Report

Inventions, patent applications, and/or licenses- Nothing to Report

Other Products - Nothing to Report

7. PARTICIPANTS & OTHER COLLABORATING ORGANIZATIONS

What individuals have worked on the project?

Name: James Funderburgh
Project Role: PI
Univ. Pitt. ID   37069
Nearest person month worked: 2.4
Contribution to Project: JLF designed the project and is directing it.

Name: Yiqin Du
Project Role: Co-investigator
Univ. Pitt. ID   82941
Nearest person month worked: 1.2
Contribution to Project: Dr. Du examined tissue for quality, carries out dissection, oversees tissue culture of the stem cells, and trains the posdoc in surgery techniques.

Name: Martha Funderburgh
Project Role: Research Specialist
Univ. Pitt. ID 37455
Nearest person month worked: 4
Contribution to Project: Ms. Funderburgh is in charge of record-keeping for human tissues, oversees regulatory approval of human and animal studies. She helps in dissection is involved in passaging and cryopreserving cells.

Name: Moira Geary
Project Role: Animal Technician
Univ. Pitt. ID 120308
Nearest person month worked: 3
Contribution to Project: Ms. Geary maintained the mouse breeding colony so that animals will be available for experiments planned for next quarter. These duties are essential even when animal work is not ongoing.

Name: Mary M. Mann
Project Role: Research Specialist
Univ. Pitt. ID 38967
Nearest person month worked: 9
Contribution to Project: Ms. Mann maintains laboratory solutions, prepares culture media and has carried out cell counts, passaging, and clonogenicity analyses of the current cell lines.

Name: Golnar Shojaati
Project Role: Research Associate
Univ. Pitt. ID 163254
Nearest person month worked: 12
Contribution to Project: Dr Shoshaati carried out animal surgery. Designed experimental approach for analysis of scarring. Designed experiments. Was first author on one manuscript and is preparing two others.

Name: Irona Khandaker
Project Role: Research Associate
Univ. Pitt. ID 170325
Nearest person month worked: 2
Contribution to Project: Dr Kandahar help with the bioinformatics analysis of RNAseq. She has designed and carried out embedding of CSSC in compressed collagen gels. She is learning animal surgery and will take over that duty for Dr Shoshaati when she leaves in November 2016.

Has there been a change in the active other support of the PD/PI(s) or senior/key personnel since the last reporting period? Nothing to report

What other organizations were involved as partners? Nothing to report

8. SPECIAL REPORTING REQUIREMENTS:

QUAD CHARTS: CY16Q3 Quad Chart in Appendix 3

Figure 1

A. Gene Upregulation by NFκ−B Activation

B. Inhibition by CoCultue With CSSC
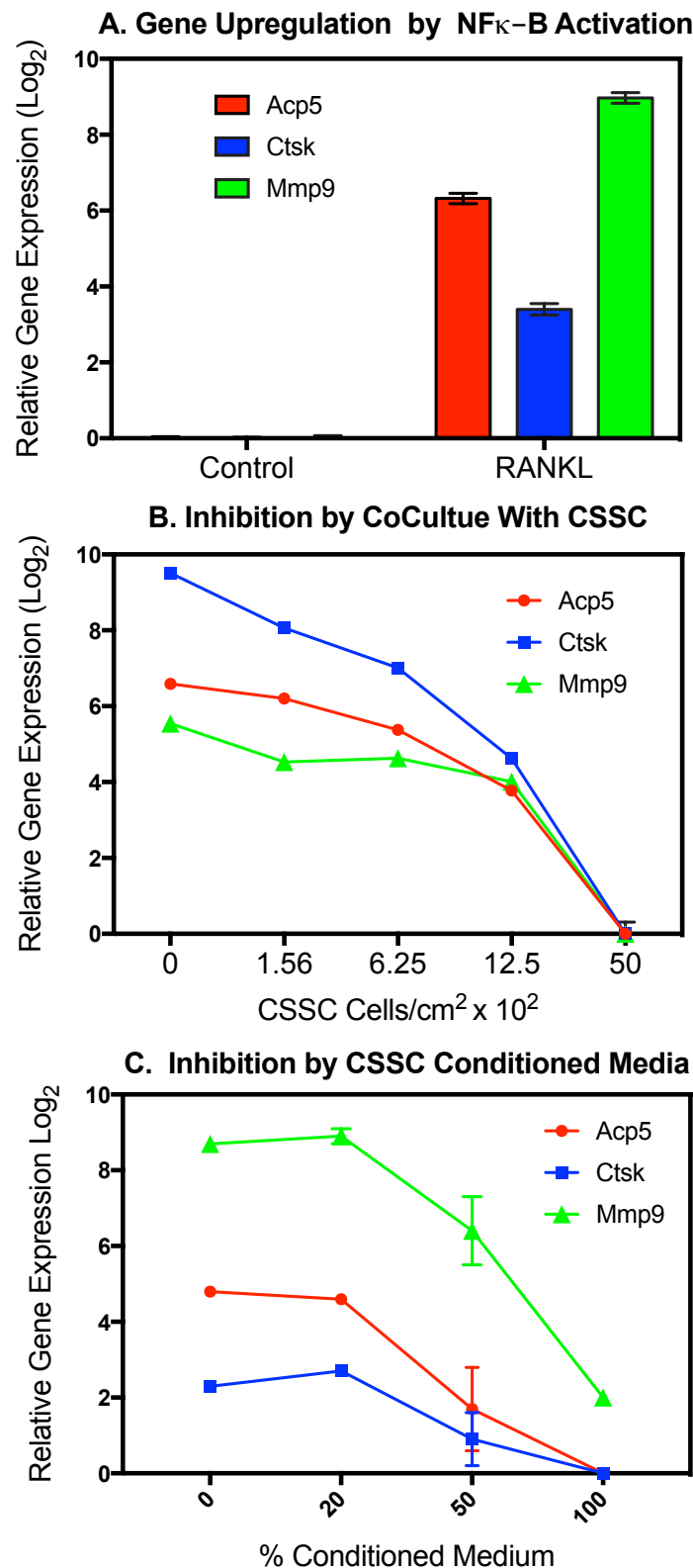

C. Inhibition by CSSC Conditioned Media

Figure 1. Assaying CSSC anti-inflammatory potential using RAW cell Activation. A. Mouse macrophage cell line RAW264.7 cells upregulate genes associated with osteoclast differentiation when inflammatory mediator NF-kappa B is stimulated with the peptide RANKL. Gene expression was measured by quantitative RT-PCR (qPCR) and is expressed relative to un-stimulated cells (Control) as Log base2 (i.e., a value of 10 represents 1024 fold up-regulation). **B.** Coculture of RAW cells with CSSC in transwells demonstrates that soluble factors from CSSC can prevent RAW cell NF-Kappa B activation. **C.** Addition of conditioned media from CSSC cultures also blocks activation of RAW cells, thus providing an assay for screening the inflammatory potential of CSSC.

Figure 2.
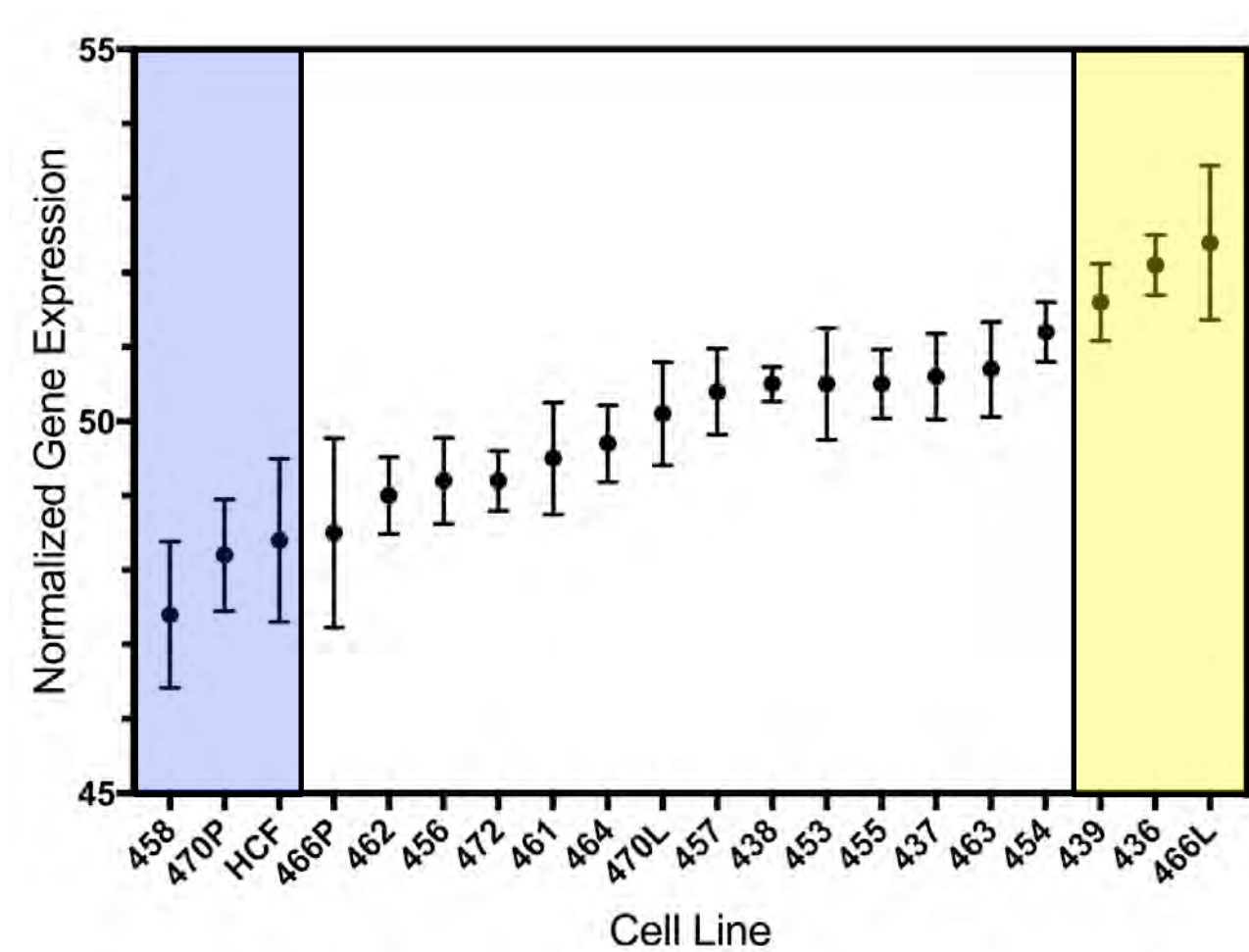
Figure 2. Ranking Stem Cell Lines. RAW 264.7 cells stimulated with RANKL, 50 ng/ml, and ConA, 20 ug/ml for 4 days were assessed for expression of genes Acp5, Mmp9, and Ctsk by qPCR as in Fig 1. Delta-Ct values for each gene were normalized and averaged to produce a gene expression score (GES). GES values of the most inhibitory lines (yellow, AIF-High: 439, 436, 466L) and of the least inhibitory lines (blue, AIF-Low: 458, 470P, HCF) were compared to the population using the Wilcox Signed Rank test and found to differ significantly (p<0.001) from the mean and from each other. These six lines were chosen for further analysis by RNAseq.
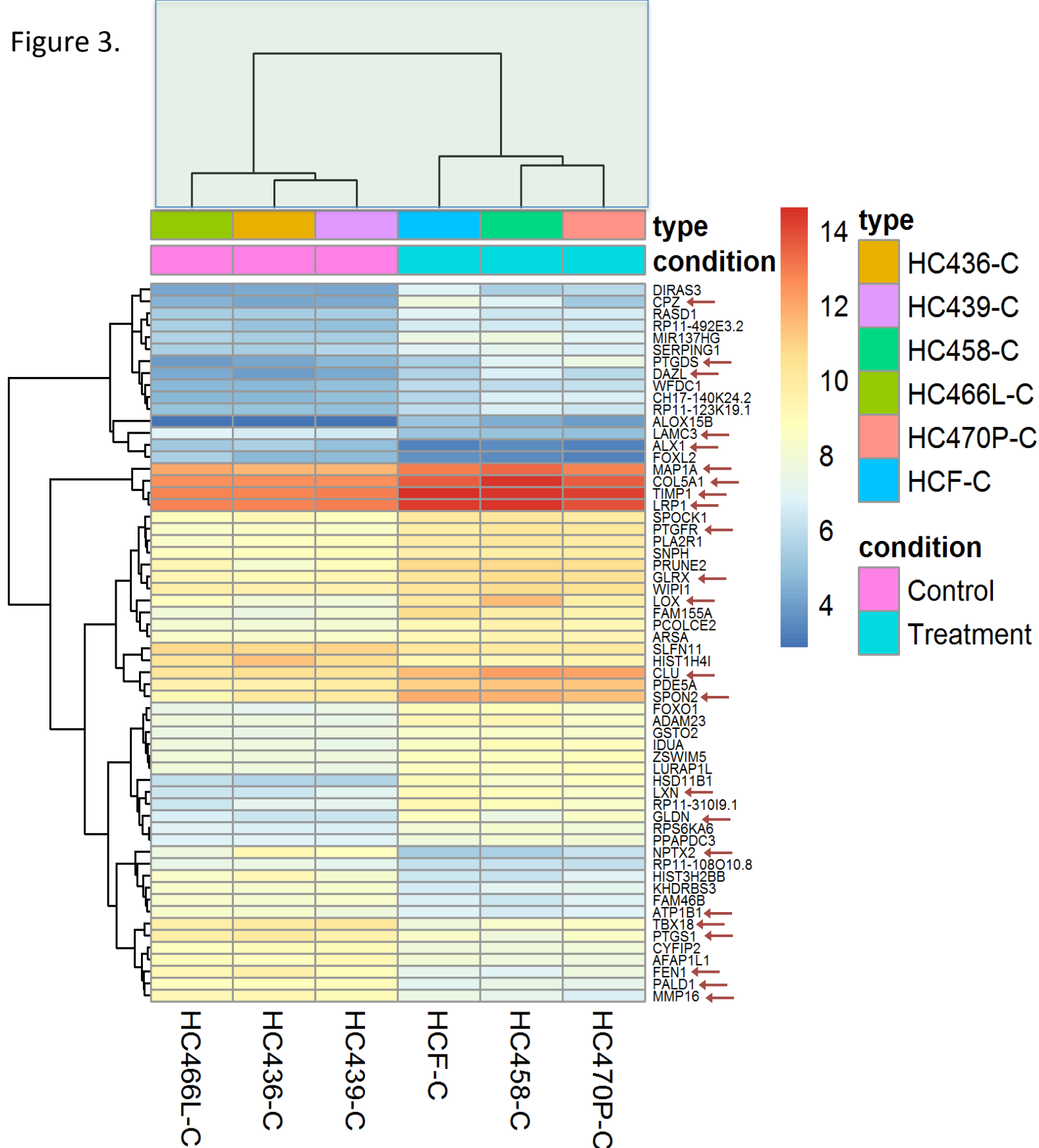
Figure 3. Cluster/Heat Map of of Expressed Genes in CSSC cell lines from six donors. **A**. Bioinformatic analysis of expressed genes identified in total cellular RNA using NGS sequencing (RNAseq) clustered the six samples into two groups based on similarity of gene expression patterns (upper shaded area). The three AIF-High cell lines (466L, 436, 439) formed a distinct grouping different from the AIF-Low lines (HCF, 458, 470P). **B** Absolute expression levels calculated as transcripts per million bases are represented on a color gradient for each cell line. Symbols of genes with statistically different expression levels between the two groups are listed on the right. RED arrows identify genes selected for qPCR analysis of all 20 lines to establish a screening assay to identify future cell lines with regenerative potential.

Table 1.

Gene	Differential Expression (log2)	P value
NPTX2	-3.80	5.4E-10
LYPD6	-2.71	7.9E-06
LAMC3	-2.69	3.1E-11
OSR2	-2.50	4.8E-05
MMP16	-2.78	3.7E-09
LEF1	-2.16	1.6E-03
HHIP	-2.67	1.5E-06
PALD1	-2.49	4.9E-14
TBX18	-2.40	4.7E-07
EID1	-2.21	6.9E-04
PTGS1	-2.19	1.2E-06
KDR	-2.15	8.1E-03
ATP1B1	-2.15	1.2E-08
SLC43A3	-2.10	7.4E-05
E2F2	-2.08	4.5E-03
COL5A1	2.05	2.5E-07
LRP1	2.14	5.7E-11
PLAT	2.16	1.1E-05
SLC1A1	2.24	4.3E-06
MDGA1	2.29	5.5E-05
CLU	2.38	9.2E-11
TIMP1	2.39	3.1E-18
PTGFR	2.42	5.3E-17
SPON2	2.59	5.2E-08
LOX	3.10	5.4E-07
GPR78	3.18	5.5E-06
PTGDS	3.36	8.8E-07
CPZ	3.46	1.7E-07
HSD11B1	4.52	1.8E-25

Table 1. Bioinformatic analysis of gene expression differences between cell lines with high and low anti-inflammatory properties. Genes marked in yellow are increased in AIF-H and blue in AIF-low. Ratio of expression is given as log base 2. P values estimate probability that the differences are valid. These genes are being tested by qPCR in multiple cell lines.
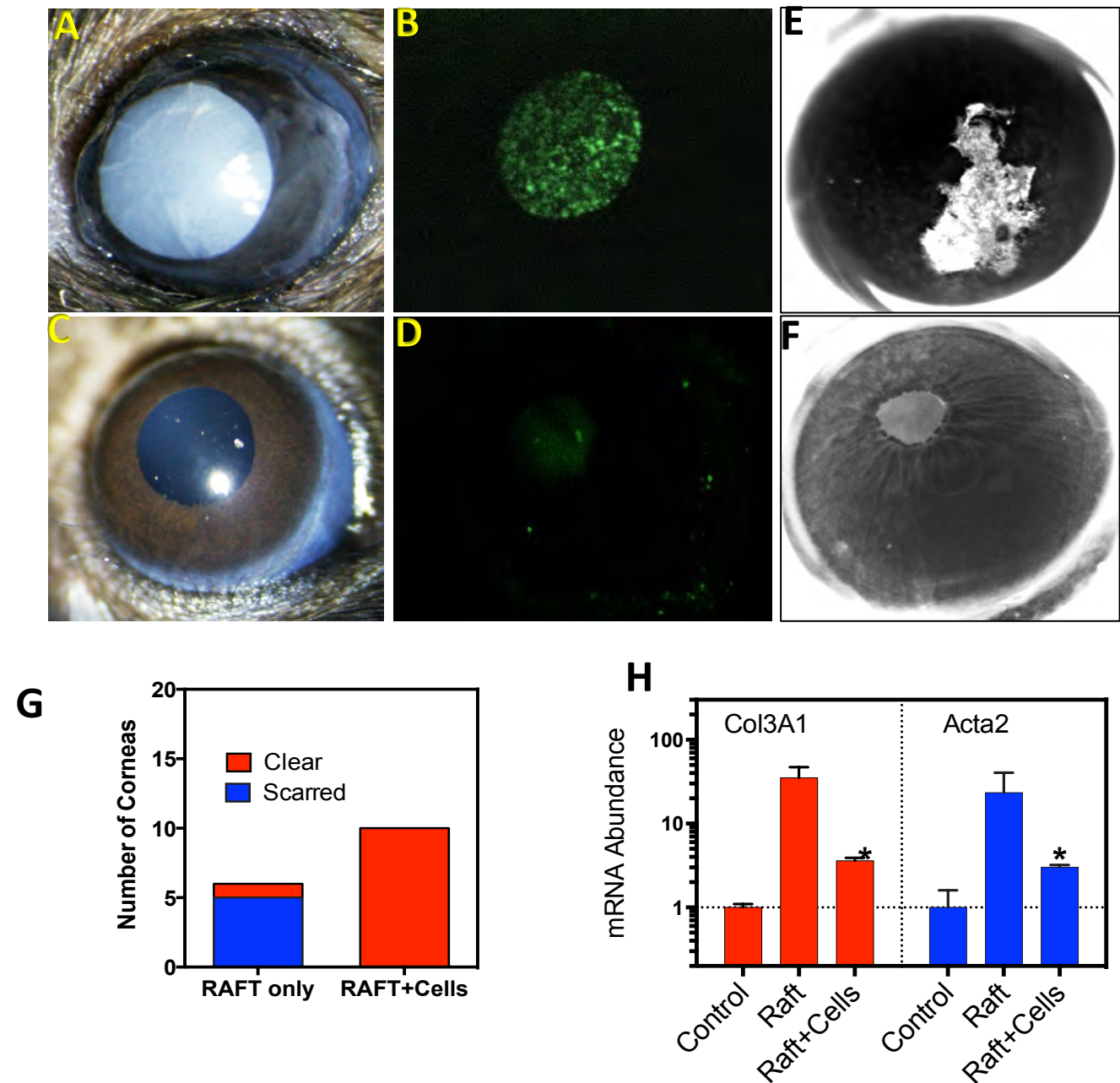
Figure 4

Figure 4 Compressed Collagen gels for stem cell-delivery. Mouse corneas were covered with a compressed plastic collagen gel (RAFT) containing corneal stromal stem cells immediately after debridement wounding (**A**). DiO stained cells could be visualized covering wound area (**B**). At 48 hr, RAFTs had dissolved (**C**). Stem cells were not visible on corneas 48 hr after wounding (**D**). At 2 weeks, corneas were scored for presence (**E**) or absence (**F**) of visible scars. Contingency table analysis showed 83% (5/6) eyes with scars with RAFT-only but no scars (0/10) after treatment with RAFT with stem cells (p<0.002, Fisher's exact test) (**G**). Expression of genes associated with fibrosis, collagen type 3 (Col3a1) and smooth muscle actin (Acta2), was significantly reduced in wounds treated with RAFT+stem cells at 2 weeks (**H**) (0<0.05, ANOVA).
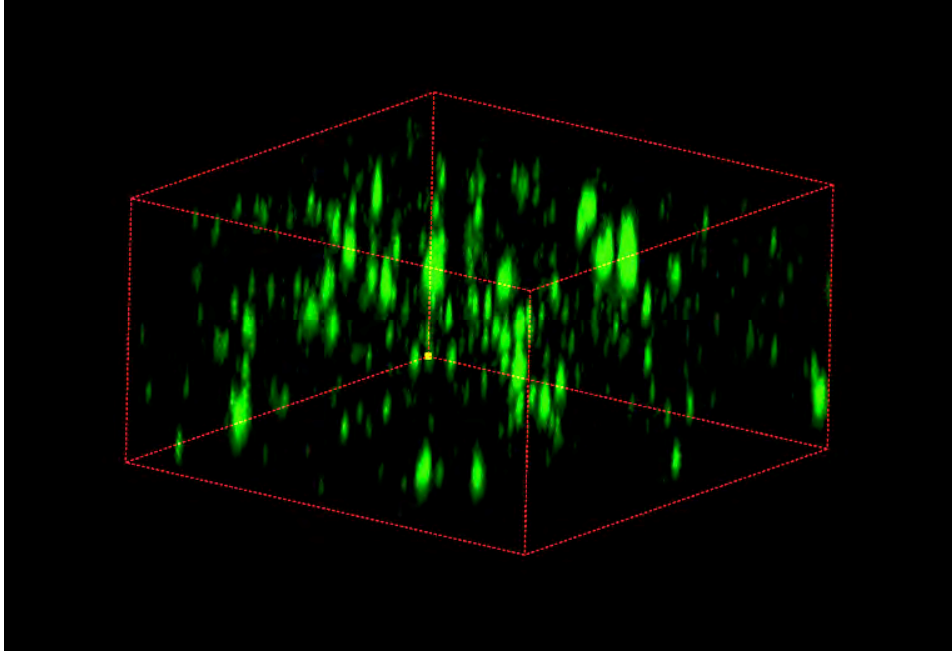
Figure 5

Figure 5   Cryopreseration of CSSC in Collagen Gels. CSSC were embedded in compressed collagen gels as in Fig 4.   These were cryopreserved in liquid nitrogen in 20% Serum/10% DMSO for 2 weeks.   The thawed material was stained with Calcein AM a dye taken up only by living cells. The presence of stained cells in the gel was imaged with confocal microscopy to provide a 3D image.   Estimates are that 50-70% of viable cells were recovered by this procedure suggesting that the ReCoBand gels can be stored for future use.

Figure 6
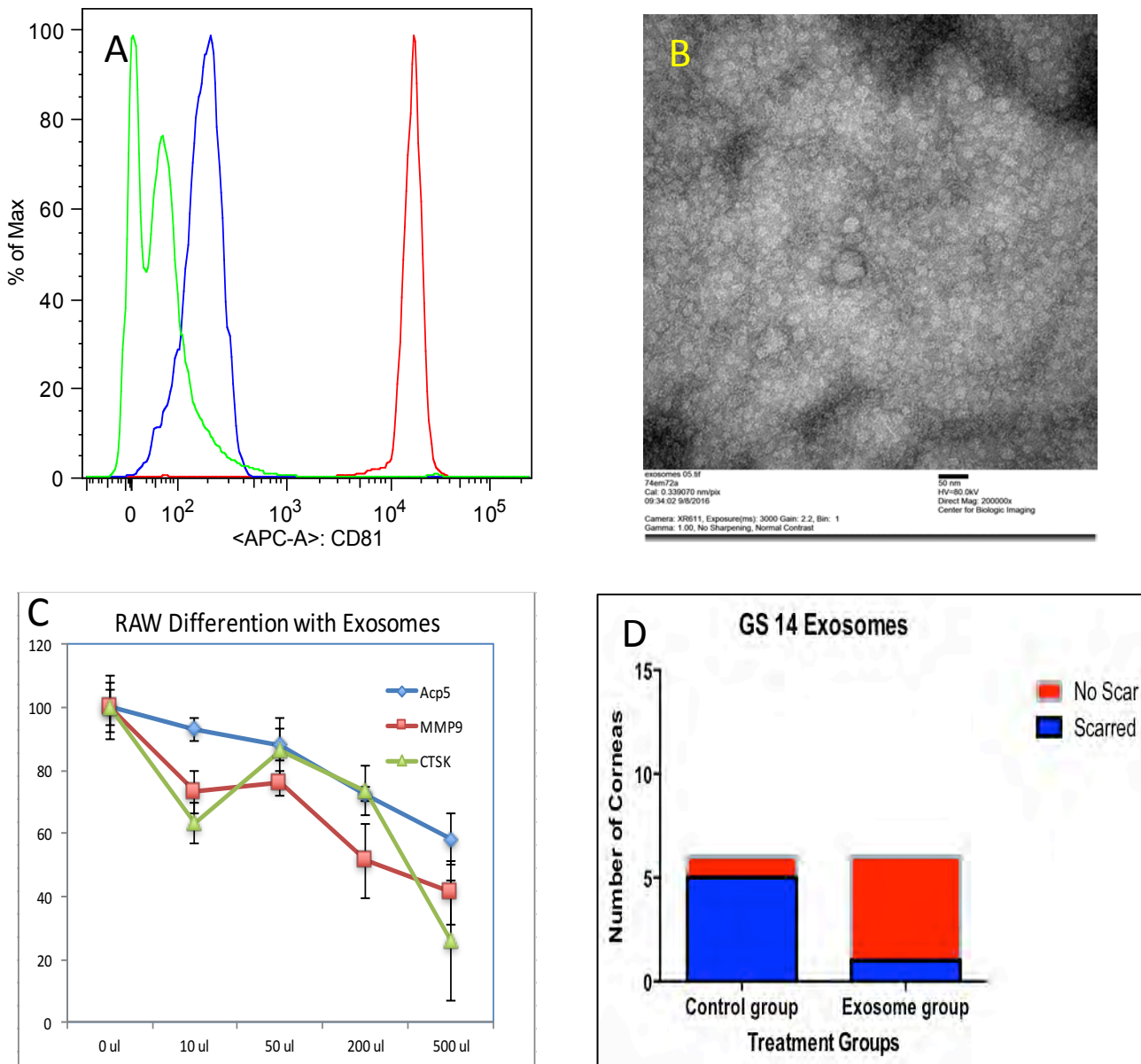
Figure 6. Exosomes from CSSC block scarring. (**A**) Flow cytometry detects CD63+/ CD81+ particles in culture media conditioned by CSSC. Anti-CD63 microbeads (green) were incubated with fresh culture media (blue) or medium conditioned by CSSC cells (red), and then detected with APC-labeled CD81 using flow cytometry. Presence of both of these antigens represents a diagnostic test for exosomes. **B.** Spherical vesicles of 20-200 nm were visualized by transmission electron microscopy after ultracentrifugation of media conditioned by CSSC. **C.** Exosomes purified from conditioned media showed a dose related inhibition of RAW cell activation by RANKL in a manner similar to the cells and conditioned media (see Fig 1). **D** Assessment of scarring (as in Fig 4) showed a statistical (p< 0.01) reduction in wounds treated with exosomes purified from CSSC conditioned media.

Early Intervention Stem Cell-Based Therapy (EISCBT) for Corneal Burns and Trauma
Log Number: MR130197   Contract # W81XWH-14-1-0465

PI: James Funderburgh   **Org:** University of Pittsburgh   **Award Amount:** $992,782
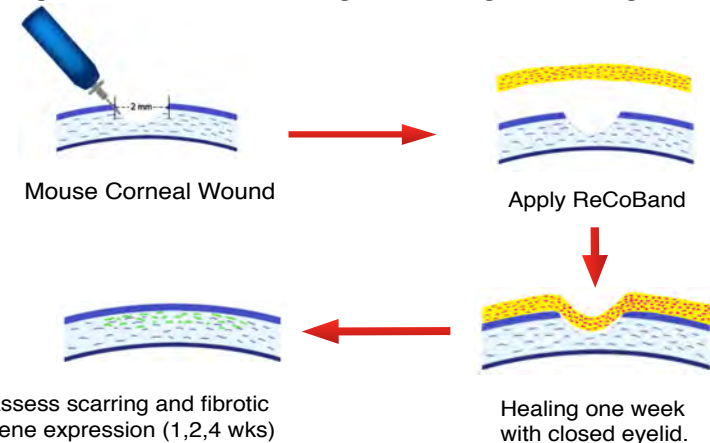
Aims

- Develop stable characterized stem cell lines to serve as a basis for EISCBT.
- Optimize a stabilized cell delivery system for corneal stromal stem cell EISCBT.
- Determine type of injury and timing for which EISCBT is most effective.

Approach.

This study will use animal models of corneal trauma and chemical burns to develop a biologic reagent that can be delivered to injured military personnel rapidly after suffering a corneal insult. The study will develop a human cell reagent and delivery system that can be rapidly translated to clinical trials.

Healing Corneal Wounds with ReCoBand:
Regenerative Corneal Bandage containing Containing Stem Cells

Mouse Corneal Wound   Apply ReCoBand

Assess scarring and fibrotic gene expression (1,2,4 wks)   Healing one week with closed eyelid.

Timeline and Cost

Activities (Tasks)	CY14	CY15	CY16	CY17
Isolation of Human Stem Cell Lines		▓		
Define Gene Markers by RNA-SEQ		▓		
Identification of Effective Cell Lines			▓	
Testing of delivery system			▓	
Demonstration of function in vivo				▓
Estimated Budget (Total $K)	**$80**	**$321**	**$334**	**$257**

Updated: (OCT 21, 2016) | = Current Location in Timeline

Goals/Milestones

CY15Q2 Isolate and passage Stem Cells Lines from Human Cadaveric Corneal Tissue. Collection to continue until 24 lines established (green box).

CY16Q2 Define markers that predict regenerative potential.

CY16Q3 Identify and cryopreserve high RP cell lines.

CY16Q4 Test delivery system and storage of ReCoBand

CY17Q3 Demonstrate functionality of the system in two in vivo models.

Comments: These goals to be accomplished by the end of the designated Quarter.

Budget Expenditure to Date: Estimate $556K

Scaffold-free tissue engineering of functional corneal stromal tissue

Scaffold-free tissue engineering of functional corneal stromal tissue

Short title: Scaffold-free engineered corneal stromal tissue

Authors:
Fatima N. Syed-Picard
Department of Ophthalmology, University of Pittsburgh

Yiqin Du
Department of Ophthalmology, University of Pittsburgh
McGowan Institute for Regenerative Medicine

Andrew J. Hertsenberg
Department of Ophthalmology, University of Pittsburgh

Rachelle Palchesko
Department of Biomedical Engineering, Carnegie Mellon University

Martha L. Funderburgh
Department of Ophthalmology, University of Pittsburgh

Adam W. Feinberg
Departments of Biomedical Engineering and Materials Science and Engineering, Carnegie Mellon University
McGowan Institute for Regenerative Medicine

Senior Author: James L. Funderburgh
Department of Ophthalmology, University of Pittsburgh
Department of Ophthalmology, Department of Cell Biology and Physiology
McGowan Institute for Regenerative Medicine
203 Lothrop St.
Pittsburgh, PA 15213
412 647 3853
412 647 5880 (FAX)
jlfunder@pitt.edu

1
2
3
Scaffold-free tissue engineering of functional corneal stromal tissue
4
5
6
Short title: Scaffold-free engineered corneal stromal tissue
7
8
9
Authors:
10
Fatima N. Syed-Picard
11
Department of Ophthalmology, University of Pittsburgh
12
13
14
Yiqin Du
15
Department of Ophthalmology, University of Pittsburgh
16
McGowan Institute for Regenerative Medicine
17
18
19
Andrew J. Hertsenberg
20
Department of Ophthalmology, University of Pittsburgh
21
22
23
Rachelle Palchesko
24
Department of Biomedical Engineering, Carnegie Mellon University
25
26
27
Martha L. Funderburgh
28
Department of Ophthalmology, University of Pittsburgh
29
30
31
Adam W. Feinberg
32
Departments of Biomedical Engineering and Materials Science and Engineering,
33
Carnegie Mellon University
34
McGowan Institute for Regenerative Medicine
35
36
37
Senior Author: James L. Funderburgh
38
Department of Ophthalmology, University of Pittsburgh
39
40
Department of Ophthalmology, Department of Cell Biology and Physiology
41
McGowan Institute for Regenerative Medicine
42
203 Lothrop St.
43
Pittsburgh, PA 15213
44
412 647 3853
45
412 647 5880 (FAX)
46
jlfunder@pitt.edu
47
48
49
50
56
57
58
59
60

Abstract

Blinding corneal scarring is predominately treated with allogeneic graft tissue, however, there is a worldwide shortage of donor tissue leaving millions in need of therapy. Human corneal stromal stem cells (CSSC) have been shown produce corneal tissue when cultured on nanofiber scaffolding, but this tissue cannot be readily separated from the scaffold. In this study, scaffold-free tissue engineering methods were used to generate biomimetic corneal stromal tissue constructs that can be transplanted in vivo without introducing the additional variables associated with exogenous scaffolding. CSSC were cultured on substrates with aligned microgrooves, which directed parallel cell alignment and matrix organization, similar to the organization of native corneal stromal lamella. CSSC produced sufficient matrix to allow manual separation of a tissue sheet from the grooved substrate. These constructs were cellular and collagenous tissue sheets, approximately 4 μm thick and contained ECM molecules typical of corneal tissue including collagen types I and V and keratocan. Similar to the native corneal stroma, the engineered corneal tissues contained long parallel collagen fibrils with uniform diameter. After being transplanted into mouse corneal stromal pockets, the engineered corneal stromal tissues became transparent, and the human CSSCs continued to express human corneal stromal matrix molecules. Both in vitro and in vivo, these scaffold-free engineered constructs emulated stromal lamellae of native corneal stromal tissues. Scaffold-free engineered corneal stromal constructs represent a novel, potentially autologous, cell-generated, biomaterial with the potential for treating corneal blindness.

Key words: Cornea, scaffold-free, ocular, stem cells, cell sheet, transplantation, human cells

1. Introduction

The cornea, the anterior most ocular tissue, is composed of a complex structure that facilitates its multiple functions. The cornea acts as physical and biological barrier, protecting the eye. It transmits 99% of incident light and provides two-thirds of the refractive power of the eye to focus light onto the retina (Meek and Leonard, 1993). The cornea is comprised of three cellular layers, of which the anterior and posterior most tissues are the epithelium and endothelium, respectively. These structures are involved in providing the barrier characteristics of the cornea and in controlling corneal hydration. The corneal stroma is the center-most tissue and makes up the bulk of its structure, comprising approximately 90% of corneal mass and thickness (Levin and Adler, 2011). The stroma has a highly organized extracellular matrix facilitating its transparency. It is a lamellar structure with each lamella composed of long, tightly packed collagen fibrils that extend the full diameter of the cornea. These fibrils are organized in parallel, uniform in diameter and uniformly spaced to form a lattice-like structure; the direction of the collagen fibrils rotates orthogonally between adjacent lamellae (Smolin et al., 2005). The highly organized structure of collagen fibrils minimizes light scatter as it passes through the cornea, facilitating corneal transparency (Hassell and Birk, 2010). Keratocytes, resident cells of the stroma, maintain its structure during normal function; however, injury to the cornea causes keratocytes to differentiate into fibroblasts and deposit a scar tissue (Fini, 1999). Unlike in healthy stromal tissue, the extracellular matrix (ECM) in scar tissue is disorganized and opaque, therefore corneal scarring results in loss of visual acuity and sometimes blindness.

Injury, infection and disease cause bilateral corneal blindness in millions of

individuals worldwide (Whitcher et al., 2001). The predominant method of treatment,

keratoplasty, involves corneal transplantation using allogeneic tissues; however,

challenges such as limited tissue availability worldwide and potential graft rejection, limit

successful treatment, leaving millions of individuals in need of therapy (Williams et al.,

2006). Tissue engineering of corneal tissue equivalents to replace damaged or

diseased corneal structures could bypass the limitations associated with the current

methods of treatment. Ideally, these engineered tissues might be generated from

autologous cells to avoid immunological rejection or other adverse biological reactions.

Additionally, the engineered stromal tissues would need to mimic the characteristic

aligned, tightly packed collagen organization and macromolecular composition of native

tissues in order to provide the strength and transparency of native stromal tissue.

Traditional tissue engineering involves combination of cells, growth factors, and

scaffolding to facilitate formation of three-dimensional tissue equivalents. Exogenous

scaffolds can strongly influence cell behavior and tissue formation through material

chemistry, topography, and mechanical properties (Clark et al., 1991; Engler et al.,

2006; LeGeros, 2008). During development, however, cells organize appropriate

structures without the need for a 3D scaffold. A scaffold-free approach to engineer

tissue sheets has been shown useful in production of a number of tissues including

skin, periosteum, myocardium, periodontium, and corneal epithelium (Chang et al.,

2012; DuRaine et al., 2015; Liu et al., 2013; Masuda and Shimizu, 2015; Na et al.,

2013; Owaki et al., 2014). This technique involves culturing cells as a monolayer, under

conditions that promote production of extracellular matrix (ECM) to form a robust tissue

sheet (See et al., 2010). Such tissue sheets can be physically removed from substratum or released chemically from thermo-responsive polymer surfaces such as poly(N-isopropylacrylamide) (Akiyama et al., 2004). Application of such a scaffold-free approach to produce corneal stromal tissue sheets could have potential to generate engineered tissue useful for replacement of scarred corneal tissue.

Previous work from our laboratory has described a population of adult stem cells from human corneal stroma, which can be expanded in culture without losing the potential to differentiate to keratocytes (Du et al., 2005). When cultured on a 3D scaffolding of aligned polymeric nanofibers, these corneal stromal stem cells (CSSC) elaborate an ECM with properties similar to that of corneal stroma (Wu et al., 2012; Wu et al., 2013b). In vivo, these cells can restore transparency to opaque corneas in animal models and prevent scar formation after stromal trauma (Basu et al., 2014; Du et al., 2009). Furthermore, CSSC can be easily isolated from human biopsy tissues, potentially allowing autologous usage (Basu et al., 2014). Although CSSC can generate a stromal ECM in vitro with similar organization of the native corneal stromal tissue, scaffolding used in previous experiments is not transparent and cannot be separated from the cell-generated ECM (Wu et al., 2012; Wu et al., 2013b).

In our current study, CSSC were cultured on a substrate containing parallel microgrooves and found to generate scaffold-free tissue sheets that emulate the highly organized structure of native corneal stromal tissues. These engineered tissues were characterized after in vitro culture, and the ability of these constructs to become transparent, functional stromal tissue in vivo was assessed. This study provides

promising data on the potential use of engineered, scaffold-free corneal stromal tissues

as a regenerative therapy to treat corneal blindness.

2. Materials and methods

2.1 Corneal stromal stem cell isolation and culture

CSSC were isolated similar to previously described methods (Basu et al., 2014; Du et

al., 2005). Human corneo-scleral rims from donors younger than 60 years with less than

5 days of preservation were obtained from the Center for Organ Recovery and

Education (www.core.org), after central tissue had been removed for transplantation.

The rims were rinsed and residual conjunctiva, Descemet's membrane with endothelial

cell layer, and trabecular meshwork were removed. Limbal tissue was dissected from

the rim, cut into approximately 3 mm segments, and digested in 0.5 mg/ml collagenase

L solution overnight at 37 ˚C. Limbal segments were pipetted repeatedly and digested

for an additional 30-40 minutes at 37 ˚C. Digest was then filtered through a cell strainer

and the cells centrifuged at 1500 rpm for 5 minutes. The resulting CSSC were plated

onto 25 cm^2 tissue culture plastic in stem cell growth medium containing 2% (v/v)

human serum, DMEM/MCDB-201 (Sigma-Aldrich 6770), AlbuMax (ThermoFisher,

#11021029), 0.1 mM ascorbic acid-2-phosphate (Sigma-Aldrich A8960), 1X ITS

(ThermoFisher #414-045), 10 ng/mL platelet-derived growth factor (R&D Systems,

Minneapolis, MN, #520-BB), 10 ng/mL epidermal growth factor (Sigma-Aldrich E9644),

10^{-8} M dexamethasone (Sigma-Aldrich D4902), 100 IU/mL penicillin and 100 ug/mL

streptomycin and 50 U/mL gentamycin. CSSC were expanded enzymatically using

TrypLe (ThermoFisher) and passaged at clonal density (~1000 cells/cm^2). For forming

scaffold-free tissue sheets, CSSC derived from a single donor cornea were used in each separate experiment. CSSC were used at passage 2-4.

2.2 Micro-patterned substrate preparation

Micro-patterned substrates were prepared similar to previously described methods (Sun et al., 2015). Glass wafers were cleaned with 70% ethanol spin, coated with a 5 μm thick layer of SPR220.3 photoresist (MicroChem Corp) and baked at 115 °C for 90 seconds. The photoresist was covered with a transparency photomask, designed in AutoCAD to have an array of parallel lines 10 μm wide and spaced 10 μm apart, and exposed to UV light for 75 seconds followed by post baking for 90 seconds at 115 °C. Regions of photoresist blocked from the UV light were then dissolved using photoresist developer MF26A (MicroChem Corp) to form a grooved mold. Sylgard 184 polydimethylsiloxane (PDMS, Down Corning) was mixed at a 10:1 base to curing agent ratio and cast onto the molds to form 1.3 cm x 1.5 cm substrates containing 10 μm wide grooves, spaced 10 μm apart, and approximately 5 μm deep. Dimensions of PDMS substrates were verified by light microscopy using a Nikon TE2000U microscope. To promote cell adhesion, PDMS were coated with fibronectin (50 μg/ml) for 1 hr, rinsed and UV sterilized in the biosafety cabinet for an additional hour.

2.3 Scaffold-free corneal stromal sheet formation

CSSC were plated onto micro-patterned PDMS substrates at a density of 10,500 cells/cm^2 in stem cell growth medium. After 48 hours, the culture medium was switched to keratocyte differentiation medium containing Advanced Dulbecco's Modified Eagle Medium (Gibco) with 1 mM ascorbate-2-phosphate, 10 ng/ml fibroblast growth factor 2

(FGF2; Gibco), and 0.1 ng/ml transforming growth factor beta 3 (TGFß3; Sigma) (Du et al., 2007; Wu et al., 2013a). Keratocyte differentiation medium was replaced every 2-3 days for 10 days at which point a tissue sheet could be mechanically separated from the substrate. Select tissue sheets were stained with Vybrant DiI ((2Z)-2-[(E)-3-(3,3-dimethyl-1-octadecylindol-1-ium-2-yl)prop-2-enylidene]-3,3-dimethyl-1-octadecylindole; perchlorate) (ThermoFisher, V-22885), by incubation of a solution of 5 μM DiI for 30 minutes at 37˚C. Phase contrast and fluorescent images of the cell sheets were acquired using a Nikon TE2000U microscope. Tissue sheets were either fixed and characterized after this *in vitro* culture or used for *in vivo* experiments. Tissue sheets were formed from CSSC isolated from two different human donor corneas. Ten separate experiments were performed to form tissue sheets, generating 10-12 scaffold-free sheets in each experiment.

2.4 Two-photon microscopy

Tissue sheets were fixed in 4% paraformaldehyde for 20 minutes and permeabilized using 0.25% Triton X solution for 10 min. Nuclei were stained with 1 µM SYTOX green (ThermoFisher) for 10 min. Two-photon microscopy was performed using an Olympus FV 1000 multi-photon microscope in backscatter mode at wavelength of 830 nm, and the generation of second harmonic signal from aligned collagen was imaged. The samples were imaged through the depth of the sample at a step size of 2 µm.

2.5 In vivo *cell sheet transplantation*

Animal studies were approved by the University of Pittsburgh Institutional Animal Care and Use Committee and carried out according to guidelines provided in the Association for Research in Vision and Ophthalmology Resolution on the Use of Animals in Ophthalmic and Vision Research. Tissue sheets were labelled with either cell membrane dye Vybrant DiO (Benzoxazolium, 3-octadecyl-2-[3-(3-octadecyl-2(3H)-benzoxazolylidene)-1-propenyl]-, perchlorate) (ThermoFisher, V-22886) to visualize the implanted cells or 5-(4,6-dichlorotriazinyl) aminofluorescein (DTAF; Sigma D0531) to visualize implanted collagenous matrix throughout the duration of implantation. For DiO labeling, tissue sheets were incubated in a solution of 5 µM DiO for 30 minutes at 37˚C, then rinsed twice prior to implantation. For DTAF labelling, tissue sheets were incubated in 1 mg/ml DTAF in 0.2 M sodium bicarbonate for 15 minutes at 37 ˚C then washed twice prior to implantation.

After general anesthesia via ketamine/xylazine (IVX Animal Health, Inc., St. Joseph, MO), the eyes of C57BL/6 mice were anesthetized using topical 0.5% proparacaine (Falcon Pharmaceuticals, Fort Worth, TX). An intrastromal pocket was generated using a 27G needle. The needle was inserted from the corneal margin into the stroma and moved laterally to separate stromal lamellae without removing any stromal tissue. Tissue damage, inflammation, and scarring were not observed as a result of this procedure. Tissue sheets were cut using a 2 mm in diameter trephine, and tissue sheets were implanted into the intrastromal pocket using forceps and spread open to lay flat. Mice were euthanized after up to 5 weeks, and eyes were enucleated for further analysis. A total of 30 mice were used in this study. Each mouse had a tissue

sheet implanted in 1 eye. The contralateral eye in each mouse remained un-operated

and used as healthy controls.

2.6 In Vivo *Imaging and Corneal Opacity Assessment*

Mouse corneas with implanted tissue sheets and healthy, un-operated control eyes

were visualized using an Olympus SZX2-ILLT dissecting microscope, 5 weeks after

implantation to qualitatively assess corneal clarity and localize either DiO labeled cells

or DTAF labeled matrix of the implanted tissue sheet. Mice were anesthetized and

stabilized using a three-point stereotactic mouse restrainer, and eyes were lubricated

with either a drop of GenTeal Gel or Gonak (Alcon) prior to imaging.

At 1 and 5 weeks after tissue sheet implantation the mice were anesthetized and

the eyes with implanted tissue sheets and healthy, un-operated control eyes were

scanned using optical coherence tomography (OCT) as previously described(Basu et

al., 2014; Boote et al., 2012). Images were acquired using a Bioptigen SD-OCT with an

axial resolution of 4 μm and A-scan acquisition rate of 20 kHz 3.5 x 3.5 mm 250 x 250

A-scans. Custom-built macros were used to register and pre-process the volumes,

punch a central button, and digitally remove the epithelium from the corneal images

using Fiji open-source image analysis software (https://fiji.sc). MetaMorph (Molecular

Devices, Inc. version 7.7.8.0) software was used to quantify the average intensity of

voxels in the stromal tissue using a uniform threshold for segmentation as a measure of

corneal opacity.

2.7 Histology and immunostaining

After in vitro culture, tissue sheets were fixed in 4% paraformaldehyde for 20 minutes, embedded in paraffin, and cut into 5 μm thick sections. Mouse eyes, 5 weeks after tissue sheet implantation, were immersed in frozen tissue embedding medium (Tissue-Tek O.C.T Compound; Electron Microscopy Sciences), flash-frozen in isopentane chilled in liquid nitrogen, and sectioned at a thickness of 12 μm. Prior to staining, sections were fixed in either 2% paraformaldehyde for 10 minutes or chilled acetone for 5 minutes.

Immunostaining was performed using antibodies against human type I collagen (Millipore; catalog # MAB3391), keratocan (Sigma; Catalog no. HPA039321), type V collagen (Clone IE2-E4, Millipore), or human keratocan (Du et al., 2009) (kindly provided by Dr. Chia-Yang Liu). Fluorescently tagged secondary antibodies Alexa Fluor 488 anti-mouse IgG, and Alexa Fluor 488 anti-rabbit IgG, or Alexa Fluor 647 anti-rabbit were obtained from ThermoFisher. Staining was performed in parallel without primary antibody as a negative control. DAPI (diamidino-2-phenylindole, 0.5 μg/ml) was used to stain nuclei.

To obtain 3D images of intact stroma, mouse eyes were enucleated and fixed overnight in 2% paraformaldehyde. Corneas were dissected and stained with DAPI. Fluorescent images were obtained from stitched z-stacks of the whole-mounted corneas. Images of whole-mounted mouse corneas and of stained corneal sections were acquired on an inverted Olympus IX81 FluoView 1000 confocal microscope. Images were saved in the native OIB format and viewed with FIJI software.

2.8 Transmission electron microscopy

After *in vitro* culture, tissue sheets were fixed in 2.5% glutaraldehyde (Electron

Microscopy Sciences) for 1 h, post-fixed in 1% osmium tetroxide (Electron Microscopy

Sciences), and dehydrated in graded alcohol washes. The samples were then

embedded in Epon (Energy Beam Sciences) and sectioned at 70 nm thickness. The

sections were stained with 1% phosphotungstic acid (Sigma Aldrich), pH 3.2 for 10

minutes and visualized with a Jeol 1011 transmission electron microscope at 80 kV.

2.9 Statistical analysis

Corneal stromal light scatter from OCT analyses are presented as averages with error

bars representing standard deviation. Independent samples t-tests were used to

compare means using GraphPad Prism 4 software and significance was considered at

$p < 0.05$.

3. Results

3.1 Scaffold-free engineered stromal lamella-like tissue emulates structure of native

tissue

Engineering a tissue with the specialized physical and biological properties of corneal

stroma could provide an alternate to allogenic lamellar grafts for treatment of corneal

scarring. To generate tissue with characteristics similar to native structures, CSSC were

plated onto a substrate that provided topological cues to direct cell and matrix

organization. PDMS substrates were generated that contained grooves 10 μm wide,

spaced 10 μm apart, and 5 μm deep (Figure 1A and 1B).   CSSC cultured on these

substrates attached with cell bodies aligned in parallel with the surface grooves (Figure

1C and 1D). Furthermore, as these cells were induced to differentiate to keratocytes, they secreted a collagenous matrix, which exhibited parallel collagen fiber alignment as revealed by 2-photon microscopy (Figure 1E). After 10 days of culture in differentiation medium, the cells organized a tissue sheet that could be lifted from the substrate using forceps (Figure 1F).

Transmission electron micrographs of the top view of the tissue sheets show that the matrix contained long, parallel collagen fibers (Figure 2A and 2B). Cross sectional images show that the diameter of the collagen fibers were approximately uniform (Figure 2C and 2D). The average diameter of the collagen fibrils was measured as 30.87 nm ± 6.22, which is similar to the collagen fibrils found in native human corneal stromal tissues that are reported as approximately 30.8 nm (Meek and Leonard, 1993). The size distribution of the collage fibrils can be seen in Figure 2E.

In addition to the structurally similarity with stromal tissue, immunostaining showed the engineered tissues sheets to contain ECM molecules characteristic of native tissues. Type I collagen (Figure 3A), type V collagen (Figure 3B), and keratocan (Figure 3C) were found in tissue sheets after in vitro culture. These ECM matrix molecules are critical in regulating proper tissue organization in the corneal stroma.

3.2 Scaffold-free engineered stromal lamella-like tissue incorporate into mouse corneal stromal tissues in vivo

The scaffold-free engineered tissue sheets were implanted into mouse corneal stromal pockets as a single layer to investigate the effects of the in vivo microenvironment on the tissue sheet and assess potential for transparency. After 5 weeks in vivo, images of

mouse eyes qualitatively appear transparent, and labeled human cells and human

matrix originating from the transplanted tissue sheet could be clearly seen in the mouse

corneas (Figure 4A-4C). Optical coherence tomography (OCT) was used to

quantitatively assess stromal light scatter as an indicator of corneal transparency. One

week after tissue sheet transplantation, tissue sheets can still be seen in the OCT scans

(Figure 4D-E), however after 5 weeks, tissue sheets could no longer be discerned in the

images reconstructed from the scans (Figure 4F). Quantification of the light scatter

from these scans indicated a significant increase in stromal light scatter one week after

implantation compared control corneas (Figure 4G), but after 5 weeks, the light scatter

of corneal stromal tissue containing tissue sheets becomes similar to those of native un-

operated control corneas (Figure 4H). These data show that the engineered tissue

sheets become transparent in the mouse corneas.

Whole-mount confocal image stacks of transplanted mouse corneas verified that

DiO-labeled, human cells remained in mouse eyes throughout 5 week implantation

period (Figure 5A and 5B), and a cross-sectional projection of these stacks showed the

cells localized to a linear region of the central stroma (Figure 5C). Hematoxylin and

eosin staining showed that mouse corneas with implanted tissue sheet maintained a

structure similar to normal corneas (Figure 5D). Immunostaining of histological sections

of the mouse eyes using antibodies specific to human keratocan showed that the

human cells delivered in the tissue sheet continued to produce keratocan in vivo (Figure

5E), whereas the human keratocan was not detected in control eyes lacking tissue

sheets (Figure 5F). Controls performed without primary antibody produced no signal

(data not shown).   These results confirm that scaffold-free tissue sheets delivered to

the corneal stroma milieu become transparent, and the embedded cells maintain a

phenotype of differentiated keratocytes in the in vivo microenvironment.

4. Discussion

Tissue engineering of corneal tissues has been long thought to have potential to

benefit individuals suffering with corneal blindness. Currently allogeneic grafts are used

to replace scarred corneal tissue, however, worldwide there is a shortage of donated

corneal tissue. Furthermore, over time, the majority of transplanted allogeneic corneal

grafts fail (Coster and Williams, 2005; Kelly et al., 2011). In this study, we found that

engineered tissue sheets can be produced by corneal stem cells in an in vitro

environment and can be harvested free of scaffolding. These sheets exhibit the unique

structure and composition of native stromal tissues, including parallel collagen fibrils of

uniform diameter organized in tight parallel arrays and the corneal-specific proteoglycan

keratocan. After in vivo transplantation, the engineered stromal tissue incorporated into

native stroma, becoming transparent without eliciting an adverse reaction. Importantly,

we recently reported that CSSC can be isolated from human limbal biopsy tissues

(Basu et al., 2014). Therefore, the cells capable of producing the engineered stromal

tissue can potentially be collected from the same patients needing treatment. Scaffold-

free engineered stromal tissue represents an approach with significant potential to serve

as an alternative to allogeneic graft tissue to treat corneal blindness bypassing the

limitations of current therapies.

It is also worth noting that embedding new tissue in the cornea by transplantation

could be used to alter the corneal shape and its refractive properties, serving a similar

function as that of eyeglasses or contact lenses. Such ' corneal inlays', particularly if

produced from autologous tissue, might have much wider application than treatment of

scarred corneas.

In earlier work we observed that corneal cells are induced to generate a stroma-

like engineered tissue by topographical cues from the culture environment, particularly

on aligned nanofibers (Basu et al., 2014; Karamichos et al., 2014; Wu et al., 2012; Wu

et al., 2013b; Wu et al., 2014a; Wu et al., 2014b). In that environment, however,

integration of the elaborated ECM with the nanofiber mesh scaffolding prevented

separation and the acquisition of a pure engineered tissue. In the current study, we

resolved the issue of obtaining scaffold-free engineered stromal tissue by culturing

CSSC on a substratum of PDMS, with its surface cast to form parallel microgrooves

during polymerization. The engineered tissue forms with relatively weak attachment to

the two-dimensional substratum and can be lifted off manually. The PDMS substratum

is inexpensive, facile to reproduce, and can readily be scaled-up, thus this method may

be adaptable for biofabrication of corneal tissue on a commercial scale.

The corneal stroma has unique properties, which render it transparent to visible

light. These include abundant tightly-packed parallel fibrillar collagen with small uniform

fibril diameters, comprised of types I and V collagen (Hassell and Birk, 2010). Corneal

transparency is also dependent of the presence of a family of corneal keratan sulfate

proteoglycans, of which the corneal-specific protein keratocan makes up about half

(Hassell and Birk, 2010). ECM produced by CSSC contained the important stromal

macromolecules, type I and V collagens and keratocan (Fig 3) and TEM analysis

showed the collagen fibrils to be organized in a manner similar to that in the human

stroma. The diameter of the fibrils was similar to that of native human stoma, approximately 30.9 nm, suggesting this construct has the potential to function as stromal tissue.

In addition to requiring specialized matrix composition and structure, transparency of the stroma only occurs in the context a specific level of hydration provided by the pumping function of the corneal endothelium. Thus, it is not possible to assess the functional transparency of stromal tissue ex vivo. Generation of free-standing tissue sheets that were not attached to opaque polymeric scaffolding made it possible, for the first time, to test ECM made by CSSC for functional transparency by implanting them into stromal pockets of living eyes. The engineered tissue sheets were not transparent immediately in vivo but became transparent over time (Fig 4). This suggests that the corneal environment may induce some reorganization of the ECM before transparency occurs. Such reorganization could involve collagen remodeling, however, by pre-labeling collagen with DTAF, we know the original collagen from the tissue construct remained in the transparent stroma 5 weeks after implantation (Fig 4). In transmission electron micrographs of mouse corneas 5 weeks after implantation, implanted tissue was indistinguishable from the host mouse tissue (data not shown), indicating that collagen of the engineered tissues had fully incorporated into the surrounding mouse tissue. The human cells delivered via the scaffold-free tissue sheets, however, clearly remained in the tissue at 5 weeks and continued to produce human keratocan (Fig 5). These data further support the idea that scaffold-free engineered stromal tissues are capable of fully integrating into the stroma and adopting functional structures.

A number of reports have demonstrated synthesis of stroma-like matrix by corneal cells in vitro (Boulze Pankert et al., 2014; Guillemette et al., 2009; Karamichos et al., 2010; Karamichos et al., 2011; Karamichos et al., 2013; Karamichos et al., 2014; Mimura et al., 2008; Ren et al., 2008; Ruberti and Zieske, 2008). Many of these studies have used mesenchymal cells expanded from corneal stroma in serum-containing media; i.e., corneal fibroblasts. Although some of these studies report the production of a stroma-like matrix from corneal fibroblasts, several observations support the superiority of a stem-cell based approach to this task. Fibroblasts do not maintain the ability to adopt a keratocyte phenotype through many population doublings (Long et al., 2000). This results in the need to use low-passage cells, available in rather limited amounts, or to use cells from more than one donor. We have successfully expanded CSSC through >20 doublings without loss of phenotype, so that CSSC from a single donor has the potential to produce keratocytes sufficient to make $>10^4$ corneas (Du et al., 2005; Du et al., 2007). Our previous studies comparing fibroblasts and CSSC show that fibroblast-produced ECM lacks some of the critical molecular components of stroma, particularly keratan sulfate (Wu et al., 2014a; Wu et al., 2014b). Most importantly is the growing body of evidence that mesenchymal stem cells have immunosuppressive properties. We previously found that human CSSC elicit little or no inflammatory response when introduced into the mouse cornea, but that corneal fibroblasts produce T-cell infiltration, haze and rejection (Du et al., 2009). The scaffold-free tissue sheets in this study were generated from human CSSC and the resulting constructs were implanted into immunocompetent mice. Similar to our previous study, the scaffold-free tissue sheets did not induce corneal haze (Figure 4) indicating that the

engineered tissues elicited little or no infiltration of immune cells from the host .

Extrapolation of these results to a human model suggests that corneal tissues produced

by CSSC may be better tolerated immunologically than tissues produced by fibroblasts.

Although use of autologous cells may be best, in cases where autologous cells are not

available, stromal tissue produced by CSSC of allogenic tissues may be a viable

second option.

5. Conclusions

Scaffold-free tissue sheets were generated from CSSC that reproduced the highly

organized structure and molecular composition of native corneal stromal lamellae. After

transplantation into corneal stromal pockets, the engineered tissue sheets incorporated

into surrounding tissues and became transparent without eliciting any adverse reaction.

The data support the idea that scaffold-free engineered stromal constructs could be

used as an autologous, cell-generated biomaterial for regenerative therapies to treat

corneal blindness.

References:

Akiyama Y, Kikuchi A, Yamato M, Okano T (2004). Ultrathin poly(N-isopropylacrylamide) grafted layer on polystyrene surfaces for cell adhesion/detachment control. Langmuir : the ACS journal of surfaces and colloids 20(13):5506-5511.

Basu S, Hertsenberg AJ, Funderburgh ML, Burrow MK, Mann MM, Du Y et al. (2014). Human limbal biopsy-derived stromal stem cells prevent corneal scarring. Sci Transl Med 6(266):266ra172.

Boote C, Du Y, Morgan S, Harris J, Kamma-Lorger CS, Hayes S et al. (2012). Quantitative assessment of ultrastructure and light scatter in mouse corneal debridement wounds. Invest Ophthalmol Vis Sci 53(6):2786-2795.

Boulze Pankert M, Goyer B, Zaguia F, Bareille M, Perron M-C, Liu X et al. (2014). Biocompatibility and functionality of a tissue-engineered living corneal stroma transplanted in the feline eye. Invest Ophthalmol Vis Sci 55(10):6908-6920.

Chang C-H, Chen C-H, Liu H-W, Whu S-W, Chen S-H, Tsai C-L et al. (2012). Bioengineered periosteal progenitor cell sheets to enhance tendon-bone healing in a bone tunnel. Biomed J 35(6):473-480.

Clark P, Connolly P, Curtis AS, Dow JA, Wilkinson CD (1991). Cell guidance by ultrafine topography in vitro. Journal of cell science 99 (Pt 1)(73-77.

Coster DJ, Williams KA (2005). The impact of corneal allograft rejection on the long-term outcome of corneal transplantation. Am J Ophthalmol 140(6):1112-1122.

Du Y, Funderburgh ML, Mann MM, SundarRaj N, Funderburgh JL (2005). Multipotent stem cells in human corneal stroma. Stem Cells 23(9):1266-1275.

Du Y, Sundarraj N, Funderburgh ML, Harvey SA, Birk DE, Funderburgh JL (2007). Secretion and organization of a cornea-like tissue in vitro by stem cells from human corneal stroma. Invest Ophthalmol Vis Sci 48(11):5038-5045.

Du Y, Carlson EC, Funderburgh ML, Birk DE, Pearlman E, Guo N et al. (2009). Stem cell therapy restores transparency to defective murine corneas. Stem Cells 27(7):1635-1642.

DuRaine GD, Brown WE, Hu JC, Athanasiou KA (2015). Emergence of scaffold-free approaches for tissue engineering musculoskeletal cartilages. Ann Biomed Eng

43(3):543-554.

Engler AJ, Sen S, Sweeney HL, Discher DE (2006). Matrix elasticity directs stem cell lineage specification. Cell 126(4):677-689.

Fini ME (1999). Keratocyte and fibroblast phenotypes in the repairing cornea. Progress in retinal and eye research 18(4):529-551.

Guillemette MD, Cui B, Roy E, Gauvin R, Giasson CJ, Esch MB et al. (2009). Surface topography induces 3D self-orientation of cells and extracellular matrix resulting in improved tissue function. Integr Biol (Camb) 1(2):196-204.

Hassell JR, Birk DE (2010). The molecular basis of corneal transparency. Experimental eye research 91(3):326-335.

Karamichos D, Guo XQ, Hutcheon AE, Zieske JD (2010). Human corneal fibrosis: an in vitro model. Invest Ophthalmol Vis Sci 51(3):1382-1388.

Karamichos D, Hutcheon AE, Zieske JD (2011). Transforming growth factor-beta3 regulates assembly of a non-fibrotic matrix in a 3D corneal model. Journal of tissue engineering and regenerative medicine 5(8):e228-238.

Karamichos D, Rich CB, Zareian R, Hutcheon AE, Ruberti JW, Trinkaus-Randall V et al. (2013). TGF-beta3 stimulates stromal matrix assembly by human corneal keratocyte-like cells. Invest Ophthalmol Vis Sci.

Karamichos D, Funderburgh ML, Hutcheon AEK, Zieske JD, Du Y, Wu J et al. (2014). A role for topographic cues in the organization of collagenous matrix by corneal fibroblasts and stem cells. PLoS One 9(1):e86260.

Kelly TL, Williams KA, Coster DJ (2011). Corneal transplantation for keratoconus: a registry study. Arch Ophthalmol 129(6):691-697.

LeGeros RZ (2008). Calcium phosphate-based osteoinductive materials. Chem Rev 108(11):4742-4753.

Levin LA, Adler FH (2011). Adler's physiology of the eye : clinical application. 11th Edition ed.: Edingburg : Saunders/Elsevier.

Liu Y, Luo H, Wang X, Takemura A, Fang YR, Jin Y et al. (2013). In vitro construction of

scaffold-free bilayered tissue-engineered skin containing capillary networks. Biomed Res Int 2013(561410.

Long CJ, Roth MR, Tasheva ES, Funderburgh M, Smit R, Conrad GW et al. (2000). Fibroblast growth factor-2 promotes keratan sulfate proteoglycan expression by keratocytes in vitro. J Biol Chem 275(18):13918-13923.

Masuda S, Shimizu T (2015). Three-dimensional cardiac tissue fabrication based on cell sheet technology. Adv Drug Deliv Rev.

Meek KM, Leonard DW (1993). Ultrastructure of the corneal stroma: a comparative study. Biophys J 64(1):273-280.

Mimura T, Amano S, Yokoo S, Uchida S, Yamagami S, Usui T et al. (2008). Tissue engineering of corneal stroma with rabbit fibroblast precursors and gelatin hydrogels. Mol Vis 14(1819-1828.

Na S, Zhang H, Huang F, Wang W, Ding Y, Li D et al. (2013). Regeneration of dental pulp/dentine complex with a three-dimensional and scaffold-free stem-cell sheet-derived pellet. Journal of tissue engineering and regenerative medicine.

Owaki T, Shimizu T, Yamato M, Okano T (2014). Cell sheet engineering for regenerative medicine: current challenges and strategies. Biotechnol J 9(7):904-914.

Ren R, Hutcheon AE, Guo XQ, Saeidi N, Melotti SA, Ruberti JW et al. (2008). Human primary corneal fibroblasts synthesize and deposit proteoglycans in long-term 3-D cultures. Developmental dynamics : an official publication of the American Association of Anatomists 237(10):2705-2715.

Ruberti JW, Zieske JD (2008). Prelude to corneal tissue engineering - gaining control of collagen organization. Progress in retinal and eye research 27(5):549-577.

See EY-S, Toh SL, Goh JCH (2010). Multilineage potential of bone-marrow-derived mesenchymal stem cell cell sheets: implications for tissue engineering. Tissue Eng Part A 16(4):1421-1431.

Smolin G, Foster CS, Azar DT, Dohlman CH (2005). Smolin and Thoft's the cornea : scientific foundations and clinical practice. 4th ed. ed. Philadelphia Lippincott Williams & Wilkins,.

Sun Y, Jallerat Q, Szymanski JM, Feinberg AW (2015). Conformal nanopatterning of extracellular matrix proteins onto topographically complex surfaces. Nature methods 12(2):134-136.

Whitcher JP, Srinivasan M, Upadhyay MP (2001). Corneal blindness: a global perspective. Bull World Health Organ 79(3):214-221.

Williams KA, Esterman AJ, Bartlett C, Holland H, Hornsby NB, Coster DJ (2006). How effective is penetrating corneal transplantation? Factors influencing long-term outcome in multivariate analysis. Transplantation 81(6):896-901.

Wu J, Du Y, Watkins SC, Funderburgh JL, Wagner WR (2012). The engineering of organized human corneal tissue through the spatial guidance of corneal stromal stem cells. Biomaterials 33(5):1343-1352.

Wu J, Du Y, Mann MM, Yang E, Funderburgh J, Wagner WR (2013a). Bioengineering Organized, Multi-Lamellar Human Corneal Stromal Tissue by Growth Factor Supplementation on Highly Aligned Synthetic Substrates. Tissue engineering Part A.

Wu J, Du Y, Mann MM, Yang E, Funderburgh JL, Wagner WR (2013b). Bioengineering organized, multilamellar human corneal stromal tissue by growth factor supplementation on highly aligned synthetic substrates. Tissue Eng Part A 19(17-18):2063-2075.

Wu J, Du Y, Mann MM, Funderburgh JL, Wagner WR (2014a). Corneal stromal stem cells versus corneal fibroblasts in generating structurally appropriate corneal stromal tissue. Exp Eye Res 120(71-81.

Wu J, Rnjak-Kovacina J, Du Y, Funderburgh ML, Kaplan DL, Funderburgh JL (2014b). Corneal stromal bioequivalents secreted on patterned silk substrates. Biomaterials 35(12):3744-3755.

1
2
3
4
5
6
7
8
9
10
11
12
13
14
15
16
17
18
19
20
21
22
23
24
25
26
27
28
29
30
31
32
33
34
35
36
37
38
39
40
41
42
43
44
45
46
47
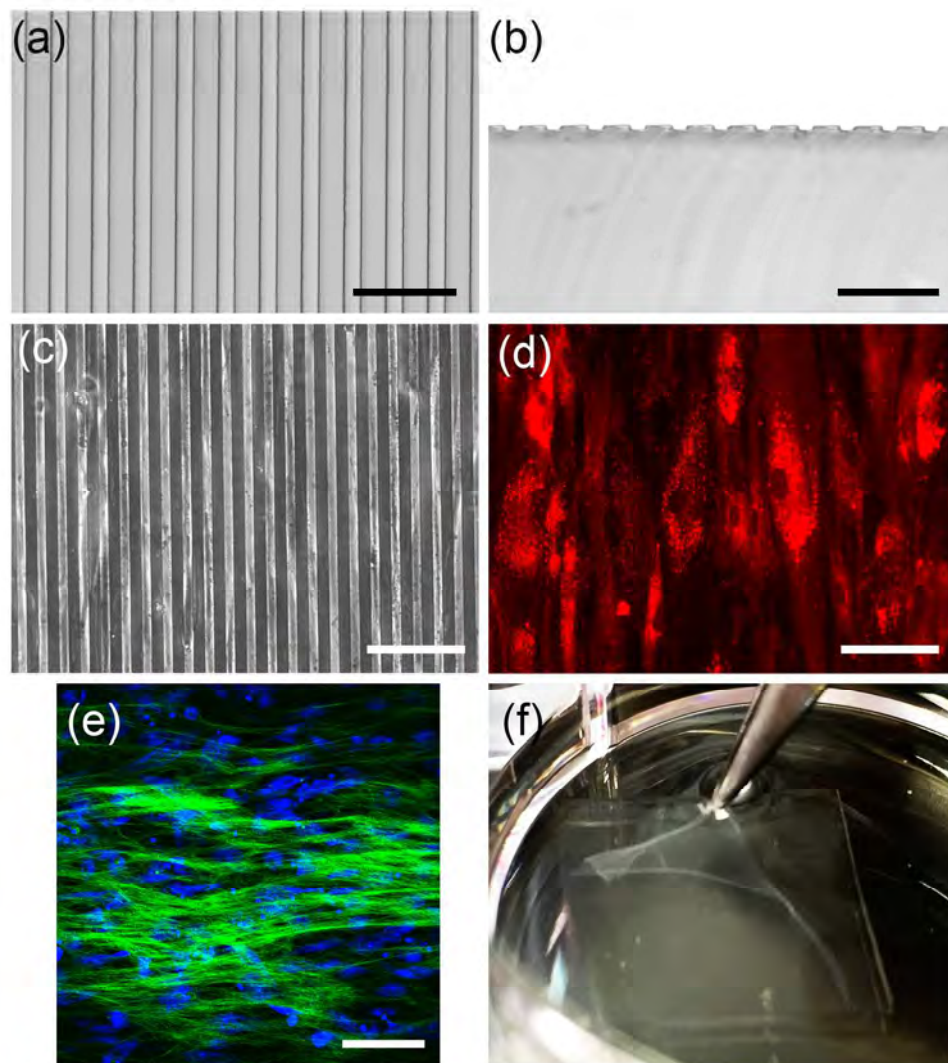48
49
50
51
52
53
54
55
56
57
58
59
60

Figure 1: Formation of scaffold-free tissue sheet with parallel cell and matrix organization. Light micrographs of (a) top view and (b) cross sectional view of the PDMS substrate show grooves approximately 10 µm wide, 10 µm apart, and 5 µm deep. (c) Phase contrast image shows CSSC cultured on the grooved substrate. (d) For better visualization, CSSC were labeled with DiI (red) and cultured on grooved substrate. (e) Two-photon micrograph of 10-day cultures of CSSC on grooved substrates in keratocyte differentiation medium (KDM) shows deposition of parallel organized collagenous matrix (green). Nuclei (blue) were stained by SYTOX-green (blue). (f) After 10 days of culture a robust tissue sheet is formed that can be separated from the substrate using forceps. Scale bars: (a) and (b) = 50 µm, (c)-(e) = 100 µm
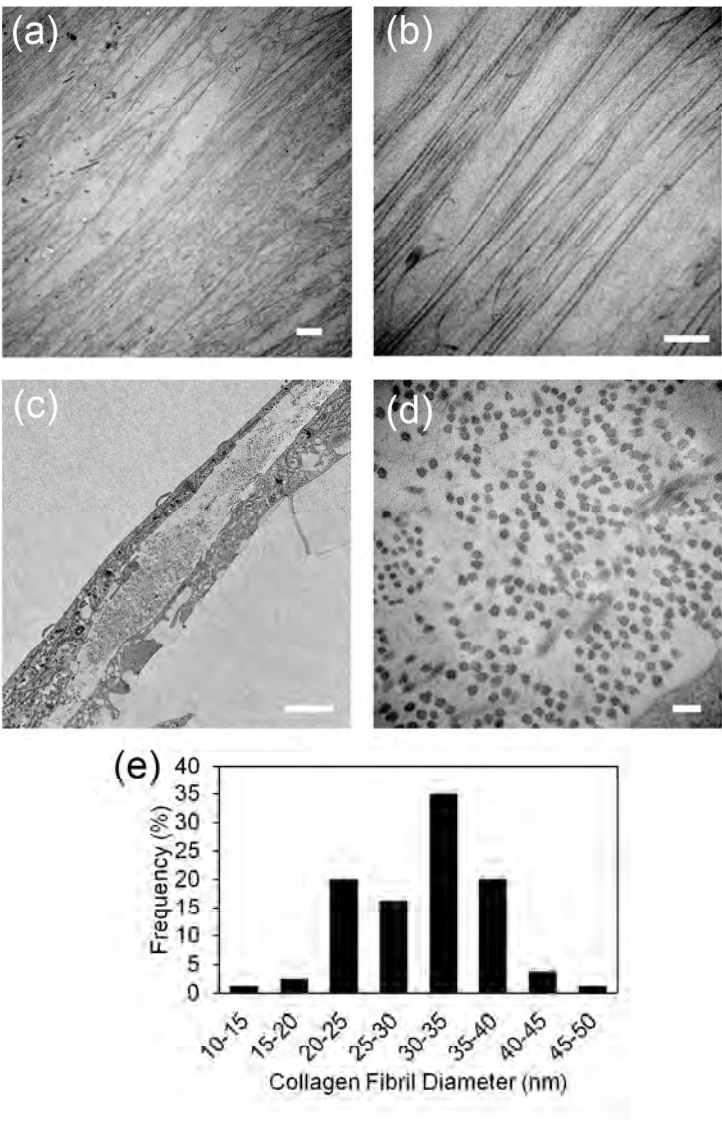
157x171mm (300 x 300 DPI)

Figure 2: Transmission electron microscopy of scaffold-free tissue sheets generated in vitro. Scaffold-free tissue sheets harvested after 12 days culture in KDM were fixed and imaged by TEM as described in Methods. (a) Lower and (b) higher magnification images of the top view of scaffold-free tissue sheets shows that the constructs contain long, parallel organized collagen fibrils. (c) Lower and (d) higher magnification images of engineered corneal stroma tissues in cross section show collagen fibrils are approximately uniform in diameter. (e) Size distribution of collagen fibril diameters as measured from TEM images of cross section of engineered tissues show that collagen fibril diameter are similar to the collagen fibril diameter seen in native, human corneal stromal tissue. Scale bars: (a) = 2 μm, (b) = 500 nm, (c) 2 μm, and (d) = 100 nm
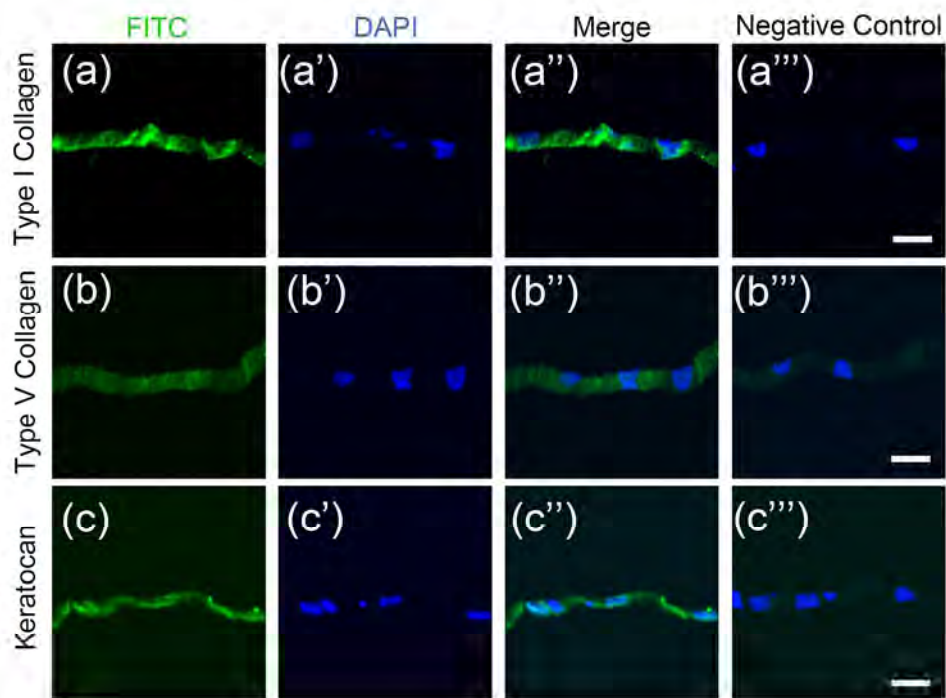
139x215mm (300 x 300 DPI)

Figure 3: Immunostaining of scaffold-free tissue sheets produced in vitro.
Paraffin sections of scaffold-free tissue sheets produced after 12 days culture in KDM were immunostained as described in Methods. (a) Presence of type I collagen (green) was detected in the matrix of scaffold-free tissue sheets, (a') with corresponding nuclear DAPI stain (blue), (a") merged image of (a) and (a'), and (a''') corresponding merged image of negative control. (b) Type V collagen expression was seen in engineered tissue sheets with (b') corresponding nuclear DAPI stain (blue), (b") merged image of (b) and (b'), and (b''') corresponding merged image of negative control. (c) Keratocan expression was detected in scaffold-free tissue sheets, with (c') corresponding nuclear DAPI stain (blue), (c") merged image of (c) and (c'), and (c''') corresponding merged image of negative control. Scale bars: 20 µm
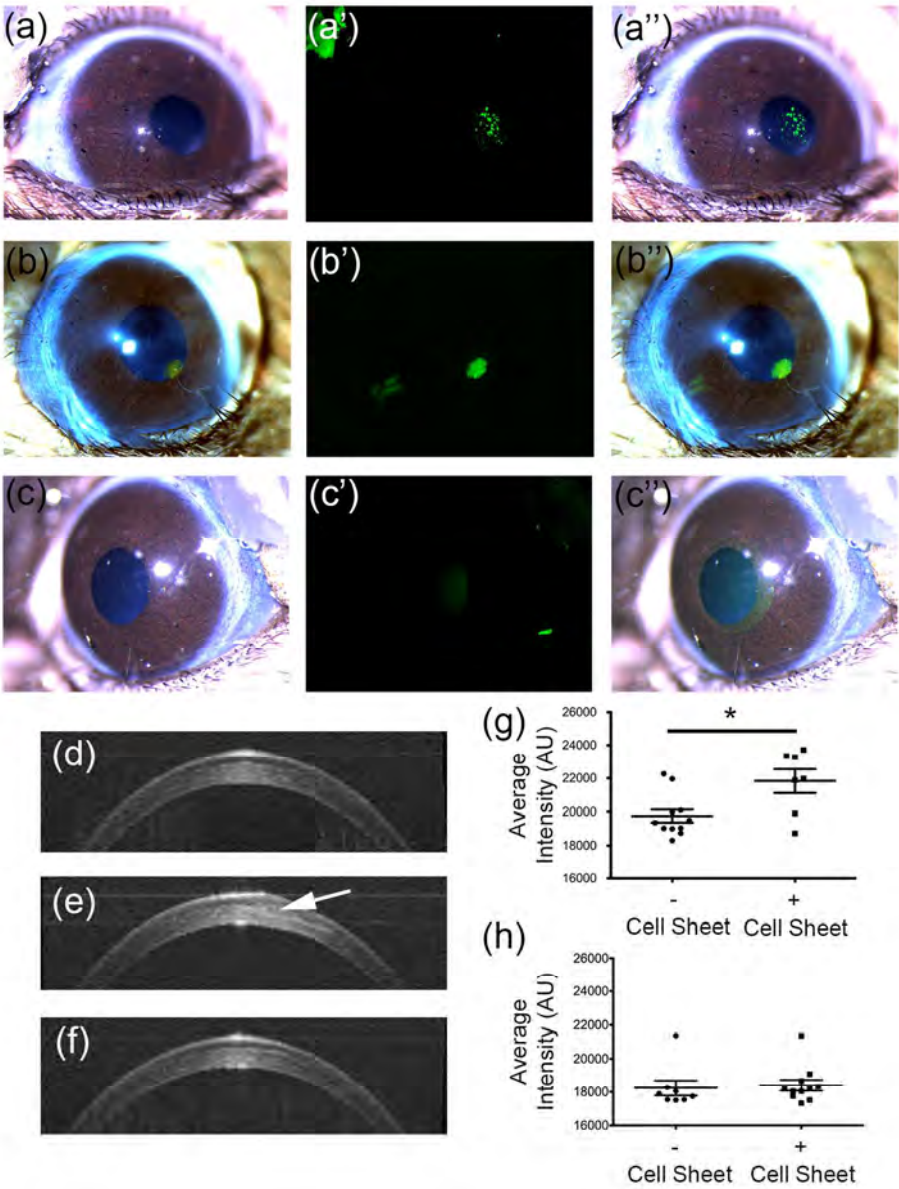
203x152mm (300 x 300 DPI)

Figure 4: Histological analysis of scaffold-free tissue sheets in mouse stromal pockets in vivo. Mouse eyes were imaged in vivo after lamellar transplantation of scaffold-free tissue sheets as described in Methods. (a) Light micrograph image of mouse eye containing scaffold-free tissue sheet with DiO-labeled cells, (a') with corresponding fluorescent image showing human cells (green), and (a'') the merged image of (a) and (a'). (b) Light micrograph image of mouse eye containing scaffold-free tissue sheet with DTAF, fluorescently-labeled matrix (green), fluorescent signal from the DTAF labeled matrix was strong enough to be seen under white light (b') with corresponding fluorescent image showing matrix (green) from scaffold-free sheet, and (b'') the merged image of (b) and (b'). (c) A light micrograph image of healthy, un-operated control mouse eye lacking a scaffold-free tissue sheet is shown, (c') with corresponding fluorescent image, and (c'') the merged image of (c) and (c'). Optical coherence tomography (OCT) was used to assess light scatter in the corneal stroma. (d) Cross-sectional projection image of untreated control mouse cornea. (e) Cross sectional image of a mouse eye with implanted tissue sheet (arrow) 1 week after implantation. (f) Cross-sectional projection image of mouse eye, 5 weeks after tissue sheet implantation. (g) Quantification of

light scatter from OCT scans of the stroma showing light scatter by implanted tissue sheet 1-week post-implantation. (h) Quantification of light scatter from OCT scans of the stroma showing light scatter by implanted tissue sheet 5-weeks post-implantation.
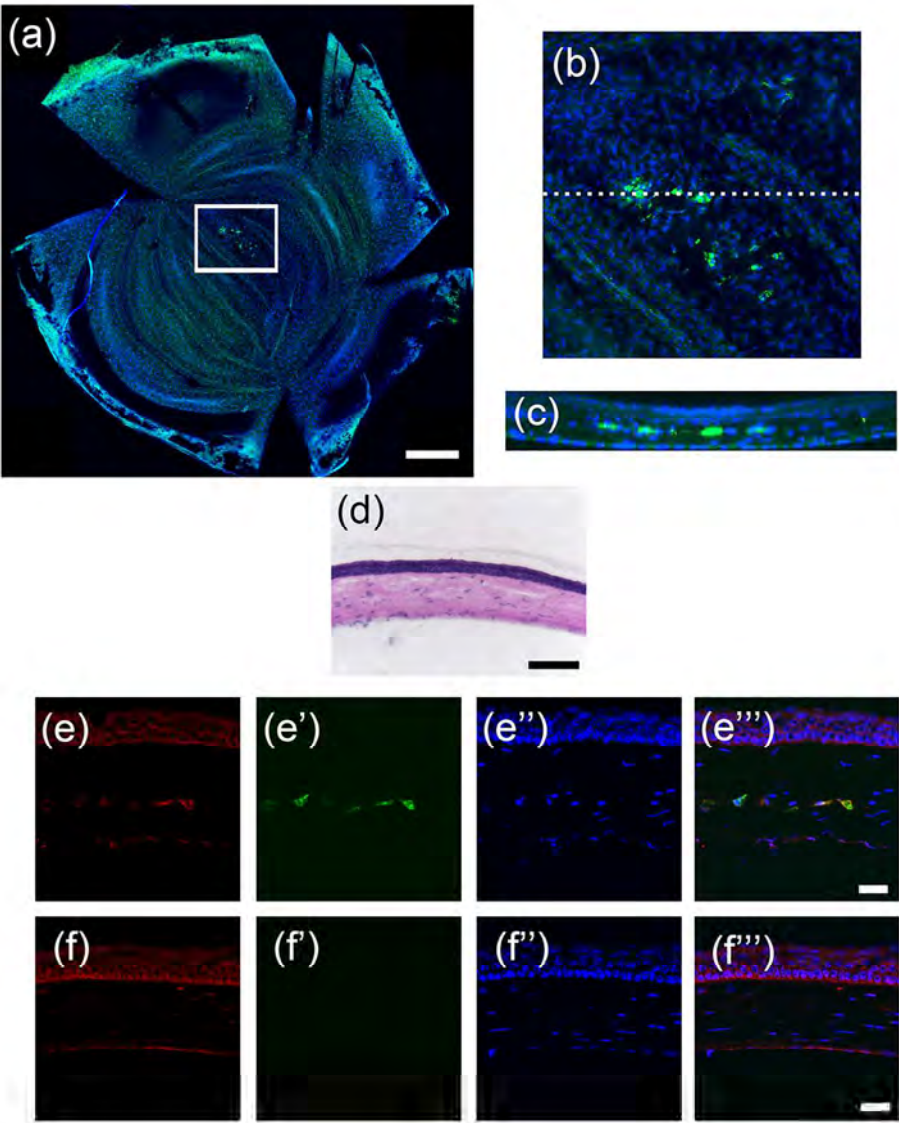
114x147mm (300 x 300 DPI)

Figure 5: Persistence of human cells and matrix in mouse cornea stroma after implantation. Five weeks after implantation of CSSC generated tissue sheets, mouse corneas were harvested and analyzed as described under Methods. (a) Confocal image of whole mount of cornea shows DiO labeled human cells (green). All cells were stained using nuclear dye DAPI (blue). Human cells are limited to boxed region, additional green signal is due to background or is non-specific. (b) Higher magnification of boxed region in (a) shows region where human cells are located and in (c) a cross sectional projection of dotted line in (b) shows that the human cells are localized to the central stroma. (d) Hematoxylin and eosin staining of mouse cornea 5 weeks after tissue sheet transplantation shows that cornea with cell sheet maintains normal structure. (e) Immunostaining human keratocan (red) in cryosections from corneas 5 weeks after tissue sheet implantation. (e') Micrograph of green channel in same region as (e) shows DiO labeled human cells (green), (e") micrograph of DAPI nuclear staining of all cells in same region as (e), and (e''') a merged image of (e)-(e") show keratocan staining localization with respect to the human cells. (f) Immunostaining human keratocan (red) in a section of control mouse cornea lacking scaffold-free tissue sheets. (f')

Micrograph of same region as (f) showing lack of DiO labeled green cells (green), (f") micrograph in same region as (f) of DAPI nuclear staining of all cells (blue), and (f''') merged image of (f)-(f"). Red signal detected in the corneal epithelial and endothelial layers is non-specific staining, also detected in negative samples lacking human cells. Scale bars: (a) = 500 μm, (b) = 100 μm, (d) = 100 μm, (e)-(f) = 20 μm

101x127mm (300 x 300 DPI)

PLOS ONE
Corneal Stromal Stem Cells Reduce Corneal Scarring by Mediating Neutrophil Infiltration after Wounding
--Manuscript Draft--

Manuscript Number:	
Article Type:	Research Article
Full Title:	Corneal Stromal Stem Cells Reduce Corneal Scarring by Mediating Neutrophil Infiltration after Wounding
Short Title:	A Role for Neutrophils in Corneal Scarring
Corresponding Author:	James L. Funderburgh, PhD University of Pittsburgh Pittsburgh, PA UNITED STATES
Keywords:	ophthalmology; cornea; wound healing; scarring; fibrosis; mesenchymal stem cells; regenerative medicine; neutrophils; TSG-6
Abstract:	Corneal scarring limits vision for millions of individuals worldwide. Corneal transplantation (keratoplasty) is the standard of care for corneal opacity but bears the risk of graft rejection and infection and is not universally available. Stem cell therapy holds promise as an alternative to keratoplasty. Stem cells from human corneal stroma (CSSC) induce regeneration of transparent corneal tissue in a mouse wound-healing model. In this study we investigated the mechanism by which CSSC prevent deposition of fibrotic tissue. Infiltration by CD11b+/Ly6G+ neutrophils and myeloperoxidase expression were increased in corneas 24 after corneal wounding but were reduced in CSSC-treated wounds. Secretion of TSG-6, a protein known to regulate neutrophil migration, was up-regulated in CSSC in response to TNFα and as CSSC differentiate to keratocytes. In vivo, wounded mouse corneas treated with CSSC contained human TSG-6. Inhibition of neutrophil infiltration into cornea by CSSC was reversed when TSG-6 expression was knocked down using siRNA. Silencing of TSG-6 expression reduced the ability of CSSC to block scarring and expression of mRNA for fibrosis-associated proteins collagen III, tenascin C, and smooth muscle actin in wounded corneas. Neutropenic mice exhibited a significant reduction in corneal scarring and fibrotic mRNA expression 2 weeks after wounding. These results support the conclusion that neutrophil infiltration is an essential event in the fibrotic response to corneal damage and that prevention of scarring by CSSC is mediated by secretion of TSG-6 by these cells.
Order of Authors:	Andrew J Hertsenberg
	Golnar Shojaati
	Martha L Funderburgh
	Mary M Mann
	Yiqin Du
	James L. Funderburgh, PhD
Opposed Reviewers:	
Additional Information:	
Question	**Response**
Financial Disclosure	
Please describe all sources of funding that have supported your work. This information is required for submission and will be published with your article, should it be accepted. A complete funding	

statement should do the following: Include **grant numbers and the URLs** of any funder's website. Use the full name, not acronyms, of funding institutions, and use initials to identify authors who received the funding. **Describe the role** of any sponsors or funders in the study design, data collection and analysis, decision to publish, or preparation of the manuscript. If the funders had **no role** in any of the above, include this sentence at the end of your statement: "*The funders had no role in study design, data collection and analysis, decision to publish, or preparation of the manuscript.*" However, if the study was **unfunded**, please provide a statement that clearly indicates this, for example: "*The author(s) received no specific funding for this work.*" * typeset	Research to Prevent Blindness, Inc. Unrestricted Grant for Vision Research. The funders had no role in study design, data collection and analysis, decision to publish, or preparation of the manuscript.
Competing Interests You are responsible for recognizing and disclosing on behalf of all authors any competing interest that could be perceived to bias their work, acknowledging all financial support and any other relevant financial or non-financial competing interests. Do any authors of this manuscript have competing interests (as described in the PLOS Policy on Declaration and Evaluation of Competing Interests)? **If yes**, please provide details about any and all competing interests in the box below. Your response should begin with this statement: *I have read the journal's policy and the authors of this manuscript have the following competing interests:* **If no** authors have any competing interests to declare, please enter this statement in the box: "*The authors have declared that no competing interests exist.*"	The authors have declared that no competing interests exist

Ethics Statement You must provide an ethics statement if your study involved human participants, specimens or tissue samples, or vertebrate animals, embryos or tissues. All information entered here should **also be included in the Methods section** of your manuscript. Please write "N/A" if your study does not require an ethics statement.	Research followed the tenets of the Declaration of Helsinki. Use of de-identified tissue samples from deceased individuals was declared not to be human subjects research by the University of Pittsburgh Institutional Review Board (IRB). Protocols were approved by the University of Pittsburgh CORID (Committee for Oversight of Research and Clinical Training Involving Decedents), Protocol #161. This study was carried out in strict accordance with the recommendations in the Guide for the Care and Use of Laboratory Animals of the National Institutes of Health and The Association for Research in Vision and Ophthalmology Statement for the Use of Animals in Ophthalmic and Vision Research. It was approved by the Institutional Animal Care and Use Committee of the University of Pittsburgh, Protocol # 15025426. Procedures were adopted to minimize pain and suffering in the animal subjects. Before wounding, mice were anesthetized by intraperitoneal injection of ketamine (50 mg/kg) and xylazine (5 mg/kg) followed by one drop of proparacaine hydrochloride (0.5%) in each eye. Animals were sacrificed by CO_2 asphyxiation in a closed chamber using a regulated flow of gas. To insure death following CO_2 exposure, secondary euthanasia was performed by cervical dislocation while the mice were under CO_2 narcosis.
Human Subject Research (involved human participants and/or tissue) All research involving human participants must have been approved by the authors' Institutional Review Board (IRB) or an equivalent committee, and all clinical investigation must have been conducted according to the principles expressed in the Declaration of Helsinki. Informed consent, written or oral, should also have been obtained from the participants. If no consent was given, the reason must be explained (e.g. the data were analyzed anonymously) and reported. The form of consent (written/oral), or reason for lack of consent, should be indicated in the Methods section of your manuscript. Please enter the name of the IRB or Ethics Committee that approved this study in the space below. Include the approval number and/or a statement indicating approval of this research.	
Animal Research (involved vertebrate animals, embryos or tissues) All animal work must have been conducted according to relevant national and international guidelines. If your study involved non-human primates, you must provide details regarding animal welfare and steps taken to ameliorate suffering; this is in accordance with the recommendations of the Weatherall report, "The use of non-human primates in research." The relevant guidelines followed and the committee that approved the study should be identified in the ethics statement.	

If anesthesia, euthanasia or any kind of animal sacrifice is part of the study, please include briefly in your statement which substances and/or methods were applied.	
Please enter the name of your Institutional Animal Care and Use Committee (IACUC) or other relevant ethics board, and indicate whether they approved this research or granted a formal waiver of ethical approval. Also include an approval number if one was obtained.	
Field Permit Please indicate the name of the institution or the relevant body that granted permission.	
Data Availability PLOS journals require authors to make all data underlying the findings described in their manuscript fully available, without restriction and from the time of publication, with only rare exceptions to address legal and ethical concerns (see the PLOS Data Policy and FAQ for further details). When submitting a manuscript, authors must provide a Data Availability Statement that describes where the data underlying their manuscript can be found. Your answers to the following constitute your statement about data availability and will be included with the article in the event of publication. **Please note that simply stating 'data available on request from the author' is not acceptable.** *If, however, your data are only available upon request from the author(s), you must answer "No" to the first question below, and explain your exceptional situation in the text box provided.* Do the authors confirm that all data underlying the findings described in their manuscript are fully available without restriction?	Yes - all data are fully available without restriction
Please describe where your data may be found, writing in full sentences. **Your answers should be entered into the box below and will be published in the form you provide them, if your manuscript is accepted.** If you are copying our sample text below, please ensure you replace any instances of XXX with the appropriate details.	All relevant data are within the paper and its Supporting Information files.

If your data are all contained within the paper and/or Supporting Information files, please state this in your answer below. For example, "All relevant data are within the paper and its Supporting Information files."

If your data are held or will be held in a public repository, include URLs, accession numbers or DOIs. For example, "All XXX files are available from the XXX database (accession number(s) XXX, XXX)." If this information will only be available after acceptance, please indicate this by ticking the box below.

If neither of these applies but you are able to provide details of access elsewhere, with or without limitations, please do so in the box below. For example:

"Data are available from the XXX Institutional Data Access / Ethics Committee for researchers who meet the criteria for access to confidential data."

"Data are from the XXX study whose authors may be contacted at XXX."

* typeset

Additional data availability information:

University of Pittsburgh

School of Medicine
Department of Ophthalmology
UPMC Eye Center
Ophthalmology & Visual Sciences Research
Center

The Eye and Ear Institute
203 Lothrop Street
Pittsburgh, PA 15213-2588
Phone: 412-647-2235
FAX: 412-647-5880

October 10, 2016

To the editors:

We are submitting a new manuscript which presents novel mechanistic insights into the process of corneal fibrosis, a major source of world blindness.

The authors wish to communicate a desire to facilitate the review and publication process in any way. Please contact us if there are any questions.

Two authors (GS and AJH) contributed equally to this work and we would like to have them both credited with first authorship.

Yours truly,

James L Funderburgh
Professor, Department of Ophthalmology,
Department of Cell Biology and Physiology
Associate Director Louis J Fox Center for Vision Restoration
McGowan Institute for Regenerative Medicine
University of Pittsburgh School of Medicine

Corneal Stromal Stem Cells Reduce Corneal Scarring by Mediating Neutrophil Infiltration after Wounding

Authors:

Andrew J. Hertsenberg[co,1]

Golnar Shojaati[co,1,2]

Martha L. Funderburgh[1]

Mary M. Mann[1]

Yiqin Du[1]

James L. Funderburgh[1,3]

Affiliation:

[1]Department of Ophthalmology, University of Pittsburgh, Pittsburgh, PA United States

[2]Department of Ophthalmology, University of Zurich, Zurich, ZH Switzerland

[3]Corresponding Author: jlfunder@pitt.edu

[co]These authors, listed alphabetically, contributed equally to this work

Abstract:

Corneal scarring limits vision for millions of individuals worldwide. Corneal transplantation (keratoplasty) is the standard of care for corneal opacity but bears the risk of graft rejection and infection and is not universally available. Stem cell therapy holds promise as an alternative to keratoplasty. Stem cells from human corneal stroma (CSSC) induce regeneration of transparent corneal tissue in a mouse wound-healing model. In this study we investigated the mechanism by which CSSC prevent deposition of fibrotic tissue. Infiltration by CD11b+/Ly6G+ neutrophils and myeloperoxidase expression were increased in corneas 24 after corneal wounding but were reduced in CSSC-treated wounds. Secretion of TSG-6, a protein known to regulate neutrophil migration, was up-regulated in CSSC in response to TNFα and as CSSC differentiate to keratocytes. In vivo, wounded mouse corneas treated with CSSC contained human TSG-6. Inhibition of neutrophil infiltration into cornea by CSSC was reversed when TSG-6 expression was knocked down using siRNA. Silencing of TSG-6 expression reduced the ability of CSSC to block scarring and expression of mRNA for fibrosis-associated proteins collagen III, tenascin C, and smooth muscle actin in wounded corneas. Neutropenic mice exhibited a significant reduction in corneal scarring and fibrotic mRNA expression 2 weeks after wounding. These results support the conclusion that neutrophil infiltration is an essential event in the fibrotic response to corneal damage and that prevention of scarring by CSSC is mediated by secretion of TSG-6 by these cells.

Introduction

Corneal blindness resulting from ocular trauma or infection affects 7-10 million people worldwide[1]. Currently the only treatment option for most of these individuals consist in corneal transplantation (lamellar or penetrating keratoplasty), a procedure complicated by tissue rejection and limited by the supply of donor tissue[2]. Consequently, there is an increasingly important need to develop alternative therapies for these patients.

Alternatives to corneal transplantation including prostheses, cell therapy, and bioengineered tissues are currently being studied with the hope of becoming the standard of care for treatment of corneal scars. Indeed, collagen-based engineered tissue has been successfully employed as partial thickness corneal grafts in animals, and is currently in human clinical trials [3-5]. Stem cells are also being investigated for use in cell therapy as well as for engineering of biosynthetic corneal tissue. Human corneal stromal stem cells (CSSC) are of particular interest for these applications as they represent the natural progenitors for keratocytes, cells that make up the corneal stroma. CSSC isolated from human limbal stromal tissue have been shown to restore transparency in a genetic model of corneal haze in mice [6-8]. These same cells have also been used to generate organized, collagenous matrices that mimic corneal tissue potentially useful as bioengineered tissue for transplant[9-11]. More recently, we have shown that limbal biopsy-derived CSSC prevent fibrotic wound healing and promote regeneration of transparent native corneal tissue in a mouse model of corneal wounding [12]. This finding could lead to the use of autologously isolated CSSC to repair damaged corneal tissue in an approach that avoids the need for donor tissue. A key to moving forward with CSSC cell therapy is to elucidate the mechanism by which these cells prevent fibrosis and scarring.

Stem cells offer the ability to regenerate damaged tissue, restoring both function and integrity. A number of studies have revealed these characteristics using multiple wound models[13-16]. It is becoming increasingly apparent that immunomodulation by stem cells is important for their anti-fibrotic/pro-regenerative wound healing properties [17-19]. Although several secreted molecules have been investigated for immunosuppressive properties, notable among them is tumor necrosis factor α stimulated gene 6 protein (TSG-6) [20-22].   TSG-6 protein is a matrikine that binds hyaluronan and other glycosaminoglycans. It is expressed by several cell types in response to inflammation[23]. TSG-6 directly inhibits neutrophil migration by binding the chemokine Interleukin-8, a neutrophil chemotactic factor[24]. TSG-6 protein, either applied topically or secreted by bone marrow mesenchymal stem cells, modulates acute-phase inflammation in corneas damaged with ethanol[25-27]. As neutrophils are the first responders to wound sites, and serve to recruit other inflammatory cells, it seems likely that preventing neutrophil infiltration at the site of injury may mediate functions of cells present in the wound at a later stages of healing.

In the present study, we investigated the mechanism by which CSSC derived from limbal biopsy tissue, prevents fibrosis in a mouse model of corneal wounding as described in previous studies[12,28]. We report that CSSC prevented infiltration of neutrophils after a stromal debridement wound in a TSG-6-dependent manner and that the absence neutrophils reduced or eliminated corneal scarring and fibrosis.

Materials and Methods

Limbal biopsy and cell culture

Human corneo-scleral rims, approved for research purposes, from de-identified donors younger than 60 years, were obtained from the Center for Organ Recovery and Education, Pittsburgh PA (www.core.org). Tissue was used within 5 days of enucleation. Research followed the tenets of the Declaration of Helsinki and was approved by the University of Pittsburgh Institutional Review Board (IRB) and CORID (Committee for Oversight of Research and Clinical Training Involving Decedents), Protocol #161. Dissection of limbal stroma was performed as described previously[12]. Briefly, rims were rinsed in Dulbecco's modified Eagle's medium (DMEM/F12) with antibiotics and an annular ring of tissue consisting of the superficial limbal epithelium and stroma, 0.5 mm into the cornea, was excised using Vannas scissors while stabilizing the tissue by holding the sclera and conjunctiva with a toothed forceps.

Excised limbal segments were incubated in collagenase (0.5 mg/ml) (Sigma-Aldrich, type L) overnight at 37 °C. Digests were triturated, incubated for an additional hour, and filtered through a 70 µm, nylon filter to obtain a single-cell suspension. Cells obtained from each segment were seeded onto a FNC (AthenaES)–coated 25 cm^2 tissue culture flask in stem cell growth medium[6] (SGM) containing 2% (v/v) pooled human serum (Innovative Research). Culture medium was changed every at 3-day intervals and cells were passaged by brief digestion with TrypLE Express (Life Technologies) when 80% confluent into a 175-cm^2 T-flask and cryopreserved at passage 1. Cells were used at passage 2 or 3. In expression studies, CSSC were cultured in SGM with 20 ng/mL TNFα or in keratocyte differentiation medium (KDM) composed of Advanced DMEM (containing GlutaMAX, Gibco, 12491), ascorbate-2-phosphate (1 mM), fibroblast growth factor–2 (10 ng/ml), and transforming growth factor–β3 (0.1 ng/ml)[9].

siRNA knockdown of TSG-6 expression

10^6 CSSC cells grown overnight in a 100 mm culture dish, were transfected with

TSG-6 siRNA (Santa Cruz Biotechnologies, sc-39819) or a scrambled control siRNA (sc-

3007), 42 nM in 9 ml SGM medium using Viromer Blue transfection agent (OriGene

Technologies) according to the manufacturer's instructions. Cells were cultured at 37º C

for 24-72 hr in the presence of TNFα (20 ng/ml) to induce TSG-6 expression. Alternately,

transfection was continued for 48 hr in SGM before CSSC were used to treat corneal

wounds. TSG-6 protein concentration in culture media was assessed using ELISA as

previously described [29].

Corneal Wounding

This study was carried out in strict accordance with the recommendations in the

Guide for the Care and Use of Laboratory Animals of the National Institutes of Health and

The Association for Research in Vision and Ophthalmology Statement for the Use of

Animals in Ophthalmic and Vision Research. It was approved by the Institutional Animal

Care and Use Committee of the University of Pittsburgh, Protocol # 15025426. Procedures

were adopted to minimize pain and suffering in the animal subjects.

Debridement procedures were done as previously described [12,28], briefly, 7-

week-old female C57BL/6 mice in groups of 5 were anesthetized by intraperitoneal

injection of ketamine (50 mg/kg) and xylazine (5 mg/kg). Our previous study and power

analysis determined that at least six eyes were required for statistical significance in visible

scar analysis and that 2 weeks provided appropriate time points for analysis of gene

expression and fibrosis[12,28]. One drop of proparacaine hydrochloride (0.5%) was added

to each eye before debridement for topical anesthesia. Corneal epithelial debridement

was performed by passing an AlgerBrush II (The Alger Company) over the central 2 mm of

the mouse cornea. Once the epithelium was removed, a second application of the AlgerBrush II was used, this time applying more pressure to remove the basement membrane and 10 to 15 μm of anterior stromal tissue. Immediately after the procedure mice received ketoprofen (3 mg/kg) for analgesia.

Fibrin gel and CSSC application

CSSC were suspended in PBS at 5×10^7 /ml and mixed 1:1 with human fibrinogen (Sigma), 70 mg/ml in PBS and maintained on ice. This concentration was determined to be the maximum number of cells that was retained on the corneal surface during healing. After wounding, 0.5 μl of thrombin (100 U/ml, Sigma) was added to the wound bed, followed immediately by 1 μl of fibrinogen (with or without CSSC). Fibrin gelled in 1 to 2 min, and a second round of thrombin and fibrinogen was applied. The wound was treated with a drop of gentamicin ophthalmic solution (0.3%). The corneal epithelium reformed over the wound in 24 to 36 hours. Eyes were examined daily for signs of rejection and infection for 1 week and weekly thereafter.

Assessment of Scarring

Two weeks after the corneal debridement all eyes were collected and the whole globes were imaged using a dissecting microscope with indirect illumination. Images of the scars were captured and scar area was determined on images of the eyes with identity of the samples masked using the Fiji open-source image analysis software package (https://fiji.sc/). Statistical analysis of the values was performed using Prism 6 (GraphPad Prism) using a one-tailed Mann-Whitney test.

Induced Neutropenia

Neutrophils were ablated in three female C57Bl/6 mice at 8 weeks of age 24 hours prior to debridement by i.p. injection of 0.5 mg, anti-Ly6G monoclonal antibody 1A8[30]. A

second dose was given at the time of debridement. Corneas were wounded as described above without fibrinogen or cellular treatment.

Quantification of neutrophil infiltration

24 hours after wounding, mice were sacrificed and eyes enucleated. Dissected corneas were cut into quarters and digested in Collagenase Type 1 (Sigma) 820 U/mL in DMEM/F12 + 10% fetal bovine serum at 37ºC for 1 hour, vortexing every 20 minutes. Digests were triturated until tissue was completely broken up and digestion continued for an additional 20 minutes. Cell suspensions were filtered through a 70 µm nylon mesh and pelleted at 340 x g for 10 minutes. Cells were stained in 50 µl staining buffer (phosphate buffered saline, 1% fetal bovine serum) by addition of Fc-Block, anti-CD45-PerCP, anti-Gr1-PE (clone RB6-8C5), and anti-CD11B-AF647 (all BD Biosciences) at 1:50 in and incubation for 30 minutes on ice in the dark. Stained cells pooled from 6 corneas were washed by centrifugation from staining buffer and fixed in 300 ul 1% paraformaldehyde in PBS before analysis by flow cytometry on a FACS Aria III Flow Cytometer (BD Biosciences). The experiment was carried out a total of 3 times.

Neutrophil Myeloperoxidase (MPO) Assay

Mouse corneas were removed and dissected 24 hr after wounding, removing all residual iris and scleral tissues, and each cornea was incised radially. Individual corneas were placed in 0.3 ml tissue extraction buffer (ThermoFisher- Life Technologies FNN0071) containing 1:100 protease inhibitor cocktail (Sigma P8340) and disrupted by sonication 4 x 30 second bursts with cooling on ice between bursts. The homogenate was centrifuged for 15 min at 14,000 x g at 4 °C. MPO activity was determined in 1:20 dilution of the homogenate using a fluorimetric immunoassay assay (R & D Systems, DY3667) according

to the manufacturer. Each sample was analyzed in triplicate and MPO was calculated

from a standard curve.

Quantitative Real Time Reverse Transcription PCR (qPCR)

6 corneas per group were dissected and pooled in 700 µl RLT extraction reagent

(Qiagen) and disrupted with MagNA Lyser green beads using 6 cycles @ 6,000 RPM with

intermittent cooling in a MagNA Lyser Instrument (Roche). The extracts centrifuged

briefly to collect lysate, and further processed using Qiashredder (Qiagen). RNA was

isolated by Qiagen Miniprep and 500 nm was transcribed to cDNA using SuperScript III

(Life Technologies) as previously described[12].   cDNA and target primers (Table 1) were

combined with SYBR Green Real-Time Master Mix (Life Technologies) and real-time

polymerase chain reaction run and data analyzed using the StepOnePlus Real-Time PCR

System (Applied Biosystems) [12]. Relative mRNA abundance was compared by $\Delta\Delta Ct$

method using 18S RNA as in internal control[12]

Table 1. PCR Primers

Gene	Protein	Accession	Primers
Acta2	smooth muscle actin	NM_007392.3	F: TGTGCTGGACTCTGGAGATG R: GAAGGAATAGCCACGCTCAG
Col3A1	collagen type III	NM_009930.2	F: CGTAAGCACTGGTGGACAGA R:CGGCTGGAAAGAAGTCTGAG
Tenc	tenascin C	NM_011607.3	F: GACTGCCCTGGGAACTGTAA R: CATAGCCTTCGAAGCACACA
TNFAIP6	TSG-6	NM_007115.3	F:AAGCACGGTCTGGCAAATACAAGC R: ATCCATCCAGCAGCACAGACATGA

Immunostaining

Immunostaining of mouse tissue was performed on 8 µm cryostat sections post-

fixed in ice-cold 4% paraformaldehyde, 70% ethanol, and 5% glacial acetic acid (v/v) for 10

minutes and blocked with 10% heat-inactivated goat or donkey serum in phosphate-

buffered saline (PBS). An antibody specific for human TSG-6 (1:150, Santa Cruz

Biotechnology) was incubated on the sections at 4 °C overnight. Slides were washed three

times in PBS and stained with AlexaFluor 546–conjugated anti-rat secondary antibody

(Life Technologies) at 1:1000 for 2 hours at room temperature. Slides were subsequently

washed three times in PBS before staining with DAPI for 15 minutes at room temperature.

Slides were imaged with an Olympus FluoView 1000 confocal microscope with a 20X oil

objective.

Results

TSG-6 *expression by CSSC.*

TSG-6 is a hyaluronan-binding protein induced by tumor necrosis factor α (TNFα) in

several different cell types including bone marrow-mesenchymal stem cells[31]. TSG-6

expression by CSSC has not been previously documented. After treatment with TNFα,

abundance of mRNA for TSG-6 in CSSC increased about 9-fold after 24 and 72 hours in

culture as measured by qPCR (Fig 1A). TSG-6 mRNA expression was also stimulated as

CSSC differentiated to keratocytes. After 72 hours in differentiation medium, TSG-6

mRNA expression was upregulated nearly 50-fold compared to undifferentiated cells

(p<0.001) (Fig 1B). Keratocan is a keratocyte-specific protein upregulated as CSSC

differentiate[32,33]. Keratocan mRNA expression was upregulated in a similar fashion to

that of TSG-6 mRNA in differentiating CSSC (Fig 1B). CSSC therefore express TSG-6 in

response to an inflammatory environment as well as during the process of differentiation

into keratocytes.

Caption for Fig 1. **TSG-6 mRNA is expressed by activated CSSC**. (**A**) CSSC

were exposed in culture to TNFα 10 ng/ml, IFN-γ 25 ng/ml (SGM-TNFα) in stem cell

growth medium (SGM) for 24 and 72 hr. mRNA for TSG-6 was detected by q-PCR as described in Methods. (**B**) CSSC were switched into keratocyte differentiation medium for 24 and 72 hr. Expression of mRNA for *TNFAIP6* (TSG-6) and *KERA* (keratocan) was determined by q-PCR. Expression levels for both genes were significantly greater than those in unstimulated cells at both time points (t-test, $p<0.05$, n=3).

Previously we showed CSSC to prevent fibrosis in mouse corneal wounds by engrafting CSSC into the stroma in fibrin gel after debridement of the epithelium and the corneal basement membrane[12]. In these treated wounds TSG-6 protein was found present in the anterior stroma four weeks after wounding (Fig 2A). This immunostaining used human-specific antibody, supporting the idea that TSG-6 protein originated from the engrafted CSSC. Eyes wounded without CSSC did not stain for TSG-6 (Fig 2B).

Caption for Fig 2 **TSG-6 accumulates in CSSC-treated wounds**. Mouse corneas were treated immediately after a debridement wound with (**A**) CSSC in fibrinogen or (**B**) fibrinogen only as described under Methods. After 7 days, cryosections of corneas were stained using antibody specific for human TSG-6 (red) and DAPI to stain cell nuclei (blue). Staining is typical of that seen in 3 different animals.

CSSC reduce neutrophil infiltration after corneal wounding.

Corneal wounding results in a rapid infiltration of neutrophils in response to mechanically-induced tissue damage[34,35]. Using flow cytometry, we identified a population of CD11b$^{+/}$ Ly6G$^+$ cells in corneal digests at 24h after wounding (Fig 3A). The application of CSSC onto the denuded stroma immediately after wounding resulted in a strong reduction of the neutrophils after the same time-period (Fig 3B).

Caption for Fig 3. **CSSC treatment reduces corneal neutrophil filtration after wounding.** Cells pooled from 6 corneas were isolated 24 hr after wounding and separated by flow cytometry as described under methods using antibodies to Ly6G and CD11b, antigens that appear on the surface of neutrophils. (**A**) Cells from wounds treated with fibrinogen only. (**B**) Cells from wounds treated with CSSC in fibrinogen. The number of cells in the positive fraction (pink circle) is shown at the base of the frame. Results represent typical data from three different experiments.

CSSC reduce corneal neutrophil infiltration via TSG-6.

TSG-6 has recently been shown *in vitro* to inhibit neutrophil migration via its interaction with Interleukin 8 [24]. The role of TSG-6 in the suppression of corneal neutrophil infiltration was tested by knockdown of TSG-6 mRNA using siRNA. Secretion of TSG-6 protein into culture media in response to TNFα was found to be completely suppressed by CSSC treated with TSG-6 siRNA (Fig 4A) (p<0.001) whereas scrambled siRNA (siCTRL) had no significant effect (Fig 4A).

The role of TSG-6 as a mediator of neutrophil infiltration was examined using CSSC in which TSG-6 secretion was knocked down. Infiltration was assessed in extracts of individual corneas by measuring MPO, a protein highly expressed in neutrophils. As shown in Fig 4B (black circles), MPO was not detected in un-wounded corneas but was elevated at 24 hr after wounding (Fig 4B, green). In wounds treated with CSSC expressing TSG-6 (CSSC-siCtrl), wounded corneas contained significantly less MPO at 24 hr (Fig 4B, blue), a value not statistically different from unwounded controls (p=0.25). However, in wounds treated with CSSC in which TSG-6 secretion was knocked down (Fig 4B, red), corneas contained MPO at the same level as untreated wounds. Suppression of neutrophil infiltration is therefore directly correlated to secretion of TSG-6 by CSSC.

Caption for Fig 4. **Knockdown of TSG-6 restores neutrophil infiltration after wounding.** Graph **(A)** shows TSG-6 in culture media detected by ELISA after 72 hr culture in stem cell growth media. Untreated CSSC, **Ctrl** (black); CSSC cultured in 20 ng/ml TNFα and 10 ng/ml IFN-γ; TNFα (blue); CSSC transfected with siRNA against TSG-6 mRNA and incubated in TNFα, IFN-γ, **siTSG-6** (red); CSSC transfected with a scrambled siRNA and incubated in TNFα, IFN-γ, **siCtrl** (green). Error bars show standard deviation (S.D.) of quadruplicate assays. Graph (**B**) shows MPO values of individual corneas as described in Methods. Error bars show S.D. and p values from double sided t-test comparing individual pairs of samples.

CSSC TSG-6 Knockdown Restores Corneal Fibrosis After Wounding.

The clinical outcome of corneal wounding is vision-impairing scarring due to corneal fibrosis. When fibrotic matrix replaces the specialized connective tissue present in corneal stroma, light is scattered resulting in vision impairment [36]. We assessed corneal fibrosis by measuring the area of visible scars and by assessing genes associated with fibrosis using qPCR at 14 days post wounding[12,28]. Corneas treated by CSSC with TSG-6 knocked down developed scars of significantly greater area compared to corneas treated with scrambled siRNA (Fig 5A). qPCR analysis of the RNA from these corneas showed increased mRNA expression for smooth muscle actin (*Act2a*), Collagen III (*Col3A*), and Tenascin C (*Tnc*) in all wounds. Wounded corneas treated with CSSC exhibited reduced expression of these mRNAs; however, knockdown of TSG-6 resulted in significantly increased expression of these genes compared with CSSC expressing TSG-6. These results, support the idea that mediation of scarring and fibrosis by CSSC is related to the ability of these cells to suppress neutrophil infiltration after wounding (Fig 5B-D).

Caption for Fig 5. **Knockdown of CSSC TSG-6 expression increases scarring and fibrosis after wounding**. (**A**) Scarred area was measured in individual eyes (n=6) as described in Methods. Eyes were treated with CSSC transfected with siRNA against TSG-6. **CSSC-siTSG-6** (blue) or with a scrambled RNA, **CSSC-siCtrl** (red). (**B,C,D**) Relative expression of fibrotic genes was measured by qPCR as described in Methods. (**B**) Act2a**; (C)** Col3a1**; (D**) Tnc. Un-wounded corneas, **No wound** (black) set to = 0. Wound without CSSC treatment, **Wound-No CSSC** (green). Wound treated with CSSC transfected with scrambled siRNA, **CSSC-siCtrl** (blue). Wound treated with CSSC transfected with siRNA against TSG-6, **CSSC-siTSG-6** (red). Error bars are S.D. of triplicates. p-values are derived from double sided t-test of pairs of data.

Neutropenia prevents fibrosis after wounding.

Neutrophil infiltration is blocked by the CSSC secretion of TSG-6; however, a direct role of neutrophils in corneal scarring has not been established. Corneal wounding consequently was carried out in mice in which a neutralizing antibody to Ly6G (clone 1A8) was injected to induce acute neutropenia [37-40]. The area of corneal scarring at 14 days was significantly reduced in the wounded neutropenic mice (Fig 6A) compared with the area of scars in control mice. The neutropenic mice also exhibited significantly reduced expression of mRNA for smooth muscle actin, collagen III, and tenascin C (Fig 6B-D) compared to that of corneas from wounded control mice. These data support the hypothesis that neutrophil involvement in corneal wounds is indeed important to the clinical outcome associated with corneal scarring.

Caption for **Fig 6. Neutropenic mice exhibit reduced corneal fibrosis.** Corneal wounds were carried out in wild type mice**, Wound Ctrl** (green), and in mice made

neutropenic by injection of anti-Ly6G antibody, as described in Methods, **Wound NP** (orange).   Area of corneal scarring (n=6) (**A**) and gene expression for fibrotic genes (**B,C,D**) were assessed at 2 weeks as in Fig 5.

Discussion

Previously, a study from this laboratory documented the ability of CSSC to prevent corneal scarring in response to corneal debridement wounds[12]. The current experiments were designed to elucidate the mechanism of this phenomenon. We found that CSSC engrafted into the wound reduced the number of neutrophils present in the cornea 24 hr after wounding. TSG-6, a protein known to prevent neutrophil migration, was secreted by the engrafted CSSC and remained in the anterior stroma for at least four weeks. Knockdown of TSG-6 expression in CSSC restored neutrophil infiltration into the wounded corneas and reduced the ability of CSSC to prevent scarring. Finally, we observed that neutropenic mice exhibited reduced scarring and fibrosis compared to wild type mice. The sum of these observations argues that alteration of corneal neutrophil infiltration by CSSC plays a key role in mediating the cellular events resulting in formation of stromal scar tissue. Such a role for neutrophils has not been previously documented in corneal wound healing, nor is it well established as a mechanism active in wound healing in other tissues such as dermis.

The mechanism by which CSSC control neutrophil infiltration appears to be secretion of TSG-6. This is consistent with reports that TSG-6 protein suppresses human neutrophil migration by interaction with the chemokine CXCL8 [24]. Mice lack CXCL8 but TSG-6 also exhibits anti-inflammatory properties in mice, suppressing corneal inflammation after chemical damage to the epithelium [26].   TSG-6 is a major contributor

to the anti-inflammatory functions of bone marrow derived mesenchymal stem cells BM-MSC [41]. CSSC are categorized as mesenchymal stem cells and share a number of properties with BM-MSC. In this study we observed that, like BM-MSC, CSSC respond to TNFα exposure with a strong upregulation of TSG-6 mRNA and protein. Interestingly, culture media containing FGF-2 and TGF-ß3, which induce keratocyte differentiation, also upregulated TSG-6 in CSSC. When CSSC are engrafted into a healing wound they differentiate to keratocytes [12], and in this study we found them to secrete TSG-6 protein into the anterior stroma (Fig 4). Knockdown of mRNA for TSG-6 in CSSC blocked their ability to inhibit neutrophil infiltration and also allowed the formation of visible scars and the upregulation of mRNA for fibrotic markers: smooth muscle actin, collagen type III, and tenascin c (Fig 5). The linkage of corneal neutrophil infiltration after wounding with subsequent scarring was confirmed in mice with neutropenia induced by injection of anti-Ly6 antibody. Neutropenic mice had greatly reduced visible scarring and fibrotic gene expression similar to unwounded controls. These results support the idea that CSSC exert their anti-fibrotic activity primarily by reducing infiltration of neutrophils, an early inflammatory response to traumatic wounding.

Cellular events in healing corneal wounds follow a temporal program typical for many other tissues. Cells near the wound site undergo apoptosis and neutrophil infiltration begins within 6 hr, peaking around 24 hr [42]. Few neutrophils remain by 72 hr. Activated tissue fibroblasts migrate into the wound site beginning 2 days after wounding and differentiation of fibroblasts to myofibroblasts begins at 3-5 days after wounding [43,44]. Expression of fibrosis-related genes is detected 2 weeks after wounding and deposition of scar tissue occurs 14-28 days after wounding [28]. This chronology shows a significant

time gap between the presence of neutrophils in the wound and deposition of scar tissue, suggesting an indirect, rather than direct, effect of the neutrophils on the fibrotic process.

Myofibroblast differentiation is a key step in the generation of corneal scars and occurs as a response of fibroblasts to TGFß [45](review). Macrophages have been proposed as a source of TGFß in wounds in several tissues [46,47]. These myeloid cells appear within 2 days after trauma but secrete TGF-ß1 during a later, resolution phase of healing which follows the appearance of myofibroblasts in the cornea [45]. Several studies support the idea that migrating corneal epithelial cells are essential for the presence of myofibroblasts in healing corneal wounds and that epithelial cells represent the source of TGFß in the healing cornea[48-51]. In neutropenic mice, corneal migration after wounding is greatly reduced and wound closure is delayed[42,52]. The implication of these two findings suggest that dysregulation of epithelial migration as a result of altered neutrophil infiltration could alter the availability of TGFß required for myofibroblast formation and scarring.

Additional effects of neutrophils may result from secretory products left behind in the wound bed by these cells. Activated neutrophils secrete several enzymes, including neutrophil elastase, a protease recently shown to induce differentiation of fibroblasts to myofibroblasts in lung tissue [53]. Neutrophil elastase is incorporated into fibrous DNA-containing structures known as neutrophil extracellular traps (NETs) which remain in tissue at least 5 days after wounds [54]. NETs localize and kill bacteria but also are found in sterile inflammation and healing wounds[55]. NETs are formed in response to a number of factors encountered in corneal wounds, including TNFα and IFN-γ[55]. NETs, like elastase, can induce myofibroblast differentiation[56]. Neutrophils also secrete fibronectin, a matrix protein absent in normal stroma, which is required for myofibroblast

differentiation[57]. These recently described properties of neutrophils are consistent with a model in which fibroblasts migrating into the wound and differentiate to myofibroblasts under the influence of TGF-ß2 secreted by epithelium and neutrophil fibronectin and elastase in NETs in the wound area. Reduction in neutrophils would alter the kinetics of TGF-ß2 secretion and the abundance of the NETs, thereby reducing the number of myofibroblasts and the secretion of fibrotic matrix.

The role of neutrophils in fibrosis is a novel concept and testing of the model proposed above may provide insight into the cellular mechanisms of corneal scarring. TSG-6, on the other hand, may not represent the sole component effecting tissue regeneration by CSSC. As seen in Fig 5, CSSC without TSG-6 expression maintain some ability to block fibrotic gene expression. Exploration of this mechanism may be clinically relevant. Only a limited proportion of individuals suffering corneal wounds will be able to obtain medical care in the brief period of time during which neutrophils populate the cornea. It is therefore important to explore the mechanism by which CSSC resolve corneal opacity in a post-inflammatory environment[6]. Understanding and enhancing this regenerative character of CSSC will allow treatment of the millions of individuals who have existing corneal opacities but no access to corneal keratoplasty.

References

1.   Mariotti SP. Global Data on Visual Impairments 2010: World Health Organization. Available from: http://www.who.int/blindness/.

2.   Thompson RW, Jr., Price MO, Bowers PJ, Price FW, Jr. Long-term graft survival after penetrating keratoplasty. Ophthalmology. 2003;110(7):1396-402. Epub 2003/07/18. doi: 10.1016/S0161-6420(03)00463-9. PubMed PMID: 12867398.

3.   Griffith M, Jackson WB, Lagali N, Merrett K, Li F, Fagerholm P. Artificial corneas: a regenerative medicine approach. Eye. 2009;23(10):1985-9. Epub 2009/01/20. doi: 10.1038/eye.2008.409. PubMed PMID: 19151645.

4.   Hackett JM, Lagali N, Merrett K, Edelhauser H, Sun Y, Gan L, et al. Biosynthetic corneal implants for replacement of pathologic corneal tissue: performance in a controlled rabbit alkali burn model. Investigative ophthalmology & visual science. 2011;52(2):651-7. Epub 2010/09/18. doi: 10.1167/iovs.10-5224. PubMed PMID: 20847116.

5.   Liu W, Merrett K, Griffith M, Fagerholm P, Dravida S, Heyne B, et al. Recombinant human collagen for tissue engineered corneal substitutes. Biomaterials. 2008;29(9):1147-58. Epub 2007/12/14. doi: 10.1016/j.biomaterials.2007.11.011. PubMed PMID: 18076983.

6.   Du Y, Carlson EC, Funderburgh ML, Birk DE, Pearlman E, Guo N, et al. Stem cell therapy restores transparency to defective murine corneas. Stem cells (Dayton, Ohio). 2009;27(7):1635-42. doi: 10.1002/stem.91. PubMed PMID: 19544455; PubMed Central PMCID: PMC2877374.

7.   Du Y, Funderburgh ML, Mann MM, SundarRaj N, Funderburgh JL. Multipotent stem cells in human corneal stroma. Stem cells (Dayton, Ohio). 2005;23(9):1266-75. doi: 10.1634/stemcells.2004-0256. PubMed PMID: 16051989; PubMed Central PMCID: PMC1941788.

8.   Du Y, Sundarraj N, Funderburgh ML, Harvey SA, Birk DE, Funderburgh JL. Secretion and organization of a cornea-like tissue in vitro by stem cells from human corneal stroma. Investigative ophthalmology & visual science. 2007;48(11):5038-45. doi: 10.1167/iovs.07-0587. PubMed PMID: 17962455; PubMed Central PMCID: PMC2874676.

9.   Wu J, Du Y, Mann MM, Yang E, Funderburgh JL, Wagner WR. Bioengineering organized, multilamellar human corneal stromal tissue by growth factor supplementation on highly aligned synthetic substrates. Tissue Eng Part A. 2013;19(17-18):2063-75. doi: 10.1089/ten.TEA.2012.0545. PubMed PMID: 23557404; PubMed Central PMCID: PMC3726016.

10.	Wu J, Du Y, Watkins SC, Funderburgh JL, Wagner WR. The engineering of organized human corneal tissue through the spatial guidance of corneal stromal stem cells. Biomaterials. 2012;33(5):1343-52. doi: 10.1016/j.biomaterials.2011.10.055. PubMed PMID: 22078813; PubMed Central PMCID: PMC3254093.

11.	Wu J, Rnjak-Kovacina J, Du Y, Funderburgh ML, Kaplan DL, Funderburgh JL. Corneal stromal bioequivalents secreted on patterned silk substrates. Biomaterials. 2014;35(12):3744-55. doi: 10.1016/j.biomaterials.2013.12.078. PubMed PMID: 24503156; PubMed Central PMCID: PMC4059021.

12.	Basu S, Hertsenberg AJ, Funderburgh ML, Burrow MK, Mann MM, Du Y, et al. Human limbal biopsy-derived stromal stem cells prevent corneal scarring. Sci Transl Med. 2014;6(266):266ra172. doi: 10.1126/scitranslmed.3009644. PubMed PMID: 25504883.

13.	Hassan WU, Greiser U, Wang W. Role of adipose-derived stem cells in wound healing. Wound repair and regeneration : official publication of the Wound Healing Society [and] the European Tissue Repair Society. 2014;22(3):313-25. Epub 2014/05/23. doi: 10.1111/wrr.12173. PubMed PMID: 24844331.

14.	Knight MN, Hankenson KD. Mesenchymal Stem Cells in Bone Regeneration. Advances in wound care. 2013;2(6):306-16. Epub 2014/02/15. doi: 10.1089/wound.2012.0420. PubMed PMID: 24527352; PubMed Central PMCID: PMC3842877.

15.	Li F, Zhao SZ. Mesenchymal stem cells: Potential role in corneal wound repair and transplantation. World journal of stem cells. 2014;6(3):296-304. Epub 2014/08/16. doi: 10.4252/wjsc.v6.i3.296. PubMed PMID: 25126379; PubMed Central PMCID: PMC4131271.

16.	Petrof G, Abdul-Wahab A, McGrath JA. Cell therapy in dermatology. Cold Spring Harbor perspectives in medicine. 2014;4(6). Epub 2014/06/04. doi: 10.1101/cshperspect.a015156. PubMed PMID: 24890834.

17.   Forbes SJ, Rosenthal N. Preparing the ground for tissue regeneration: from mechanism to therapy. Nature medicine. 2014;20(8):857-69. Epub 2014/08/08. doi: 10.1038/nm.3653. PubMed PMID: 25100531.

18.   Glenn JD, Whartenby KA. Mesenchymal stem cells: Emerging mechanisms of immunomodulation and therapy. World journal of stem cells. 2014;6(5):526-39. Epub 2014/11/27. doi: 10.4252/wjsc.v6.i5.526. PubMed PMID: 25426250; PubMed Central PMCID: PMC4178253.

19.   Wang Y, Chen X, Cao W, Shi Y. Plasticity of mesenchymal stem cells in immunomodulation: pathological and therapeutic implications. Nature immunology. 2014;15(11):1009-16. Epub 2014/10/21. doi: 10.1038/ni.3002. PubMed PMID: 25329189.

20.   Beltran SR, Svoboda KK, Kerns DG, Sheth A, Prockop DJ. Anti-inflammatory protein tumor necrosis factor-alpha-stimulated protein 6 (TSG-6) promotes early gingival wound healing: an in vivo study. Journal of periodontology. 2015;86(1):62-71. Epub 2014/10/02. doi: 10.1902/jop.2014.140187. PubMed PMID: 25269522.

21.   Liu L, Yu Y, Hou Y, Chai J, Duan H, Chu W, et al. Human umbilical cord mesenchymal stem cells transplantation promotes cutaneous wound healing of severe burned rats. PloS one. 2014;9(2):e88348. Epub 2014/03/04. doi: 10.1371/journal.pone.0088348. PubMed PMID: 24586314; PubMed Central PMCID: PMC3930522.

22.   Wang H, Chen Z, Li XJ, Ma L, Tang YL. Anti-inflammatory cytokine TSG-6 inhibits hypertrophic scar formation in a rabbit ear model. European journal of pharmacology. 2015;751C:42-9. Epub 2015/02/11. doi: 10.1016/j.ejphar.2015.01.040. PubMed PMID: 25661977.

23.   Milner CM, Day AJ. TSG-6: a multifunctional protein associated with inflammation. Journal of cell science. 2003;116(Pt 10):1863-73. Epub 2003/04/15. doi: 10.1242/jcs.00407. PubMed PMID: 12692188.

24.   Dyer DP, Thomson JM, Hermant A, Jowitt TA, Handel TM, Proudfoot AE, et al. TSG-6 inhibits neutrophil migration via direct interaction with the chemokine CXCL8.

Journal of immunology. 2014;192(5):2177-85. Epub 2014/02/07. doi: 10.4049/jimmunol.1300194. PubMed PMID: 24501198; PubMed Central PMCID: PMC3988464.

25.   Oh JY, Lee RH, Yu JM, Ko JH, Lee HJ, Ko AY, et al. Intravenous mesenchymal stem cells prevented rejection of allogeneic corneal transplants by aborting the early inflammatory response. Molecular therapy : the journal of the American Society of Gene Therapy. 2012;20(11):2143-52. Epub 2012/08/30. doi: 10.1038/mt.2012.165. PubMed PMID: 22929658; PubMed Central PMCID: PMC3498800.

26.   Oh JY, Roddy GW, Choi H, Lee RH, Ylostalo JH, Rosa RH, Jr., et al. Anti-inflammatory protein TSG-6 reduces inflammatory damage to the cornea following chemical and mechanical injury. Proceedings of the National Academy of Sciences of the United States of America. 2010;107(39):16875-80. Epub 2010/09/15. doi: 10.1073/pnas.1012451107. PubMed PMID: 20837529; PubMed Central PMCID: PMC2947923.

27.   Qi Y, Jiang D, Sindrilaru A, Stegemann A, Schatz S, Treiber N, et al. TSG-6 released from intradermally injected mesenchymal stem cells accelerates wound healing and reduces tissue fibrosis in murine full-thickness skin wounds. The Journal of investigative dermatology. 2014;134(2):526-37. Epub 2013/08/08. doi: 10.1038/jid.2013.328. PubMed PMID: 23921952.

28.   Boote C, Du Y, Morgan S, Harris J, Kamma-Lorger CS, Hayes S, et al. Quantitative assessment of ultrastructure and light scatter in mouse corneal debridement wounds. Investigative ophthalmology & visual science. 2012;53(6):2786-95. doi: 10.1167/iovs.11-9305. PubMed PMID: 22467580; PubMed Central PMCID: PMC3367468.

29.   Ylostalo JH, Bartosh TJ, Tiblow A, Prockop DJ. Unique characteristics of human mesenchymal stromal/progenitor cells pre-activated in 3-dimensional cultures under different conditions. Cytotherapy. 2014;16(11):1486-500. Epub 2014/09/19. doi: 10.1016/j.jcyt.2014.07.010. PubMed PMID: 25231893; PubMed Central PMCID: PMCPMC4190045.

30.   Daley JM, Thomay AA, Connolly MD, Reichner JS, Albina JE. Use of Ly6G-specific monoclonal antibody to deplete neutrophils in mice. Journal of leukocyte biology. 2008;83(1):64-70. Epub 2007/09/22. doi: 10.1189/jlb.0407247. PubMed PMID: 17884993.

31.   Lee TH, Wisniewski HG, Vilcek J. A novel secretory tumor necrosis factor-inducible protein (TSG-6) is a member of the family of hyaluronate binding proteins, closely related to the adhesion receptor CD44. The Journal of cell biology. 1992;116(2):545-57. Epub 1992/01/01. PubMed PMID: 1730767; PubMed Central PMCID: PMC2289279.

32.   Carlson EC, Liu CY, Chikama T, Hayashi Y, Kao CW, Birk DE, et al. Keratocan, a cornea-specific keratan sulfate proteoglycan, is regulated by lumican. The Journal of biological chemistry. 2005;280(27):25541-7. Epub 2005/04/26. doi: 10.1074/jbc.M500249200. PubMed PMID: 15849191; PubMed Central PMCID: PMC2874675.

33.   Tasheva ES, Funderburgh JL, Corpuz LM, Conrad GW. Cloning, characterization and tissue-specific expression of the gene encoding bovine keratocan, a corneal keratan sulfate proteoglycan. Gene. 1998;218(1-2):63-8. Epub 1998/09/30. PubMed PMID: 9751803.

34.   O'Brien TP, Li Q, Ashraf MF, Matteson DM, Stark WJ, Chan CC. Inflammatory response in the early stages of wound healing after excimer laser keratectomy. Archives of ophthalmology (Chicago, Ill : 1960). 1998;116(11):1470-4. Epub 1998/11/21. PubMed PMID: 9823348.

35.   Wilson SE, Mohan RR, Mohan RR, Ambrosio R, Jr., Hong J, Lee J. The corneal wound healing response: cytokine-mediated interaction of the epithelium, stroma, and inflammatory cells. Progress in retinal and eye research. 2001;20(5):625-37. Epub 2001/07/27. PubMed PMID: 11470453.

36.   Hassell JR, Birk DE. The molecular basis of corneal transparency. Experimental eye research. 2010;91(3):326-35. doi: 10.1016/j.exer.2010.06.021. PubMed PMID: 20599432; PubMed Central PMCID: PMC3726544.

37.   Han Y, Cutler JE. Assessment of a mouse model of neutropenia and the effect of an anti-candidiasis monoclonal antibody in these animals. The Journal of infectious diseases. 1997;175(5):1169-75. Epub 1997/05/01. PubMed PMID: 9129081.

38.   Norman KE, Cotter MJ, Stewart JB, Abbitt KB, Ali M, Wagner BE, et al. Combined anticoagulant and antiselectin treatments prevent lethal intravascular coagulation. Blood. 2003;101(3):921-8. Epub 2002/10/24. doi: 10.1182/blood-2001-12-0190. PubMed PMID: 12393622.

39.   Tate MD, Brooks AG, Reading PC, Mintern JD. Neutrophils sustain effective CD8(+) T-cell responses in the respiratory tract following influenza infection. Immunology and cell biology. 2012;90(2):197-205. Epub 2011/04/13. doi: 10.1038/icb.2011.26. PubMed PMID: 21483446.

40.   Tateda K, Moore TA, Deng JC, Newstead MW, Zeng X, Matsukawa A, et al. Early recruitment of neutrophils determines subsequent T1/T2 host responses in a murine model of Legionella pneumophila pneumonia. Journal of immunology. 2001;166(5):3355-61. Epub 2001/02/24. PubMed PMID: 11207291.

41.   Lee RH, Yu JM, Foskett AM, Peltier G, Reneau JC, Bazhanov N, et al. TSG-6 as a biomarker to predict efficacy of human mesenchymal stem/progenitor cells (hMSCs) in modulating sterile inflammation in vivo. Proceedings of the National Academy of Sciences of the United States of America. 2014;111(47):16766-71. Epub 2014/11/12. doi: 10.1073/pnas.1416121111. PubMed PMID: 25385603; PubMed Central PMCID: PMC4250139.

42.   Li Z, Burns AR, Smith CW. Two waves of neutrophil emigration in response to corneal epithelial abrasion: distinct adhesion molecule requirements. Investigative ophthalmology & visual science. 2006;47(5):1947-55. Epub 2006/04/28. doi: 10.1167/iovs.05-1193. PubMed PMID: 16639002.

43.   Zieske JD, Guimaraes SR, Hutcheon AE. Kinetics of keratocyte proliferation in response to epithelial debridement. Experimental eye research. 2001;72(1):33-9. Epub 2001/01/03. doi: 10.1006/exer.2000.0926. PubMed PMID: 11133180.

44.   Matsuba M, Hutcheon AE, Zieske JD. Localization of thrombospondin-1 and myofibroblasts during corneal wound repair. Experimental eye research. 2011;93(4):534-40. Epub 2011/07/14. doi: 10.1016/j.exer.2011.06.018. PubMed PMID: 21749870; PubMed Central PMCID: PMCPMC3206171.

45.   Saika S, Yamanaka O, Okada Y, Sumioka T. Modulation of Smad signaling by non-TGFbeta components in myofibroblast generation during wound healing in corneal stroma. Experimental eye research. 2016;142:40-8. Epub 2015/12/18. doi: 10.1016/j.exer.2014.12.015. PubMed PMID: 26675402.

46.   Wahl SM, McCartney-Francis N, Allen JB, Dougherty EB, Dougherty SF. Macrophage production of TGF-beta and regulation by TGF-beta. Annals of the New York Academy of Sciences. 1990;593:188-96. Epub 1990/01/01. PubMed PMID: 1695824.

47.   Ishida Y, Gao JL, Murphy PM. Chemokine receptor CX3CR1 mediates skin wound healing by promoting macrophage and fibroblast accumulation and function. Journal of immunology. 2008;180(1):569-79. Epub 2007/12/22. PubMed PMID: 18097059.

48.   Hutcheon AE, Guo XQ, Stepp MA, Simon KJ, Weinreb PH, Violette SM, et al. Effect of wound type on Smad 2 and 4 translocation. Investigative ophthalmology & visual science. 2005;46(7):2362-8. Epub 2005/06/28. doi: 10.1167/iovs.04-0759. PubMed PMID: 15980223.

49.   Zieske JD, Hutcheon AE, Guo X, Chung EH, Joyce NC. TGF-beta receptor types I and II are differentially expressed during corneal epithelial wound repair. Investigative ophthalmology & visual science. 2001;42(7):1465-71. Epub 2001/05/31. PubMed PMID: 11381048.

50.   Wilson SE, Mohan RR, Hutcheon AE, Mohan RR, Ambrosio R, Zieske JD, et al. Effect of ectopic epithelial tissue within the stroma on keratocyte apoptosis, mitosis, and myofibroblast transformation. Experimental eye research. 2003;76(2):193-201. Epub 2003/02/05. PubMed PMID: 12565807.

51.   Stramer BM, Zieske JD, Jung JC, Austin JS, Fini ME. Molecular mechanisms controlling the fibrotic repair phenotype in cornea: implications for surgical outcomes.

Investigative ophthalmology & visual science. 2003;44(10):4237-46. PubMed PMID: 14507867.

52.   Marrazzo G, Bellner L, Halilovic A, Li Volti G, Drago F, Dunn MW, et al. The role of neutrophils in corneal wound healing in HO-2 null mice. PloS one. 2011;6(6):e21180. Epub 2011/06/23. doi: 10.1371/journal.pone.0021180. PubMed PMID: 21695050; PubMed Central PMCID: PMCPMC3117875.

53.   Gregory AD, Kliment CR, Metz HE, Kim KH, Kargl J, Agostini BA, et al. Neutrophil elastase promotes myofibroblast differentiation in lung fibrosis. Journal of leukocyte biology. 2015;98(2):143-52. Epub 2015/03/07. doi: 10.1189/jlb.3HI1014-493R. PubMed PMID: 25743626; PubMed Central PMCID: PMCPMC4763951.

54.   McIlroy DJ, Jarnicki AG, Au GG, Lott N, Smith DW, Hansbro PM, et al. Mitochondrial DNA neutrophil extracellular traps are formed after trauma and subsequent surgery. Journal of critical care. 2014;29(6):1133.e1-5. Epub 2014/08/17. doi: 10.1016/j.jcrc.2014.07.013. PubMed PMID: 25128442.

55.   Liu FC, Chuang YH, Tsai YF, Yu HP. Role of neutrophil extracellular traps following injury. Shock (Augusta, Ga). 2014;41(6):491-8. Epub 2014/05/20. doi: 10.1097/shk.0000000000000146. PubMed PMID: 24837201.

56.   Chrysanthopoulou A, Mitroulis I, Apostolidou E, Arelaki S, Mikroulis D, Konstantinidis T, et al. Neutrophil extracellular traps promote differentiation and function of fibroblasts. The Journal of pathology. 2014;233(3):294-307. Epub 2014/04/18. doi: 10.1002/path.4359. PubMed PMID: 24740698.
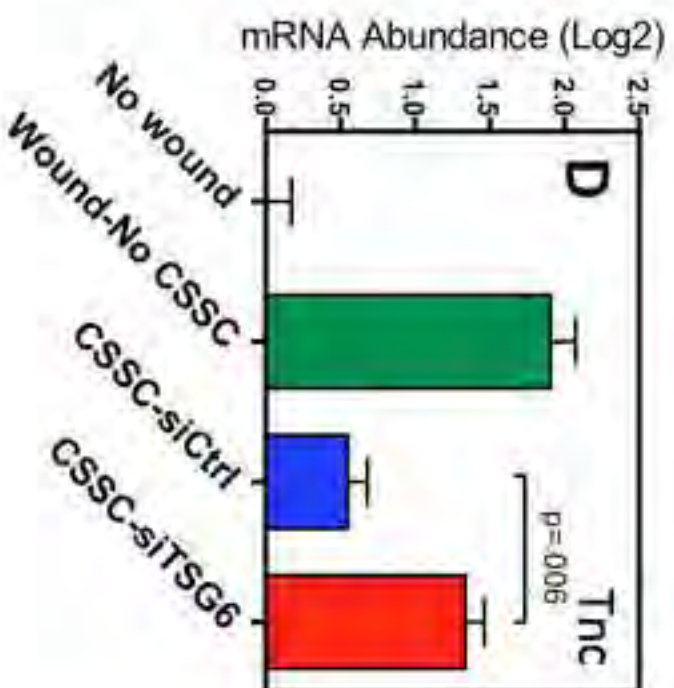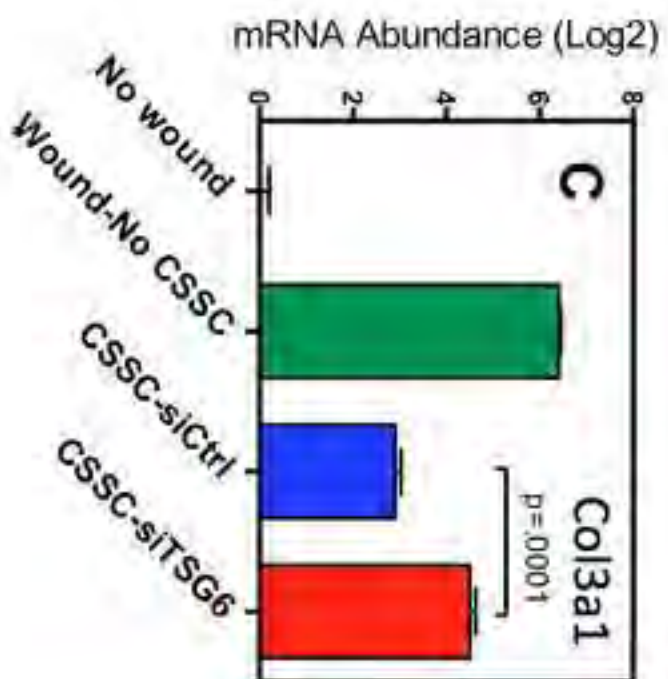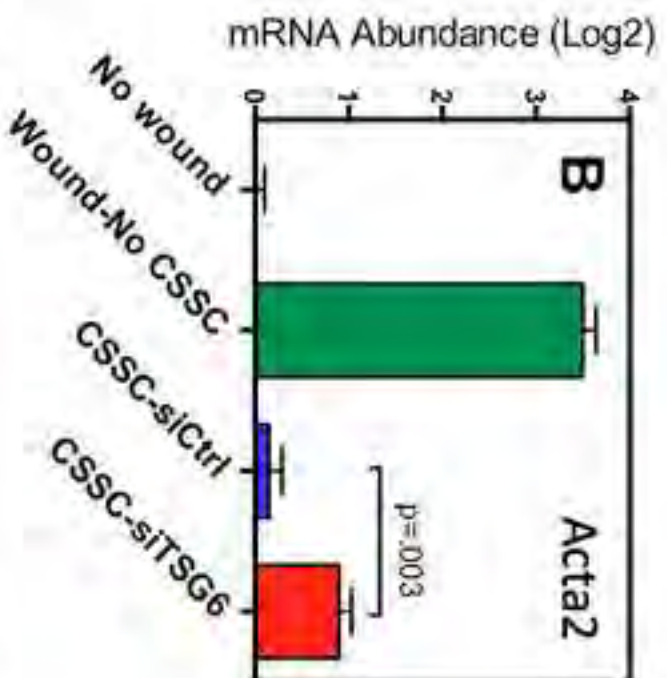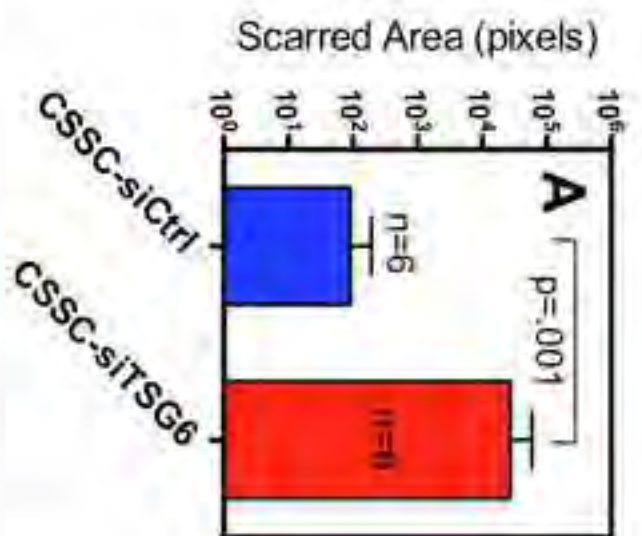
57.   Bastian OW, Koenderman L, Alblas J, Leenen LP, Blokhuis TJ. Neutrophils contribute to fracture healing by synthesizing fibronectin+ extracellular matrix rapidly after injury. Clinical immunology (Orlando, Fla). 2016;164:78-84. Epub 2016/02/09. doi: 10.1016/j.clim.2016.02.001. PubMed PMID: 26854617.
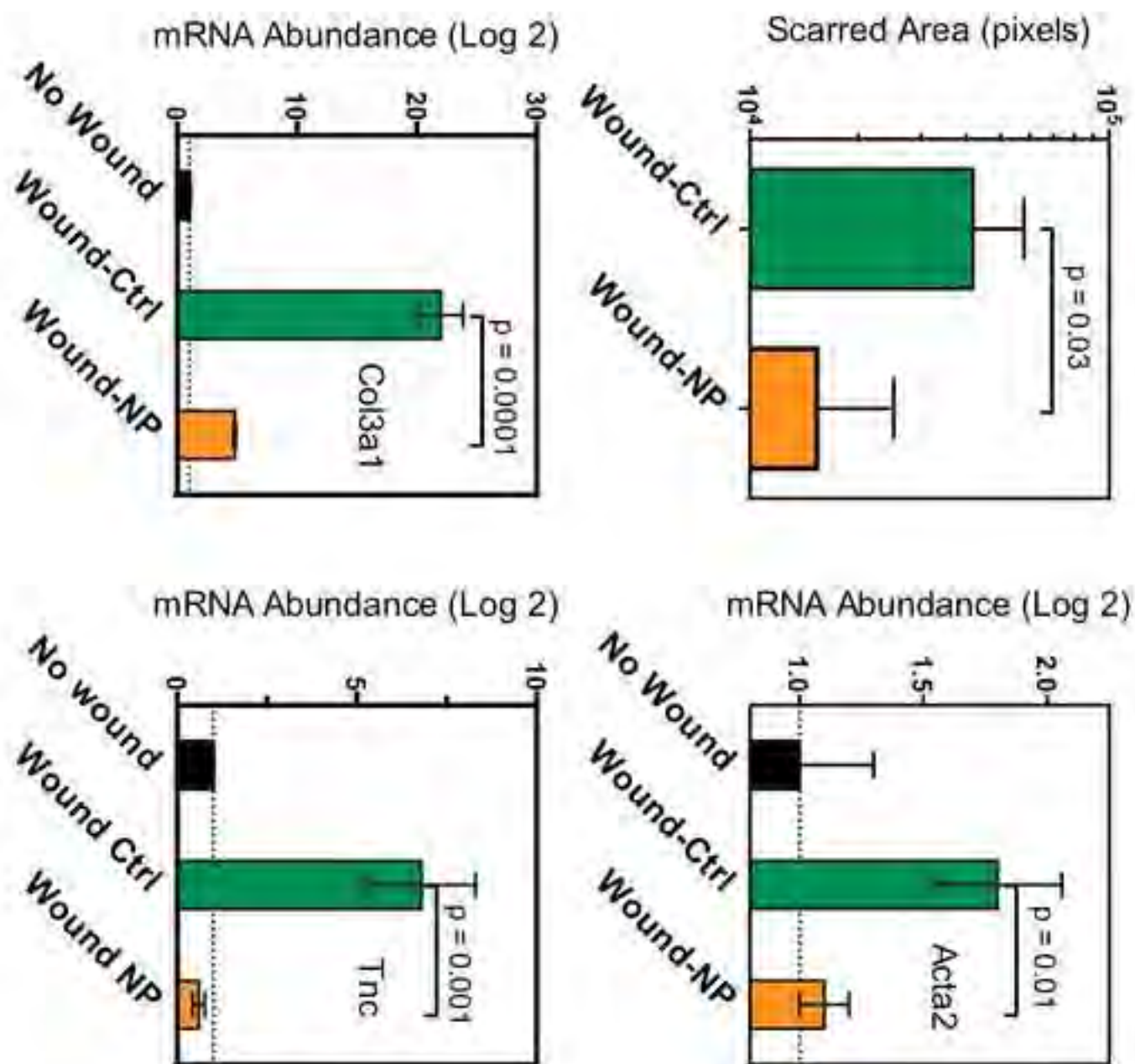
Fig1

Fig2

A — TSG-6 — Wound+ CSSC

B — TSG-6 — Wound Only

Fig3

Fig4

Fig5

Fig6
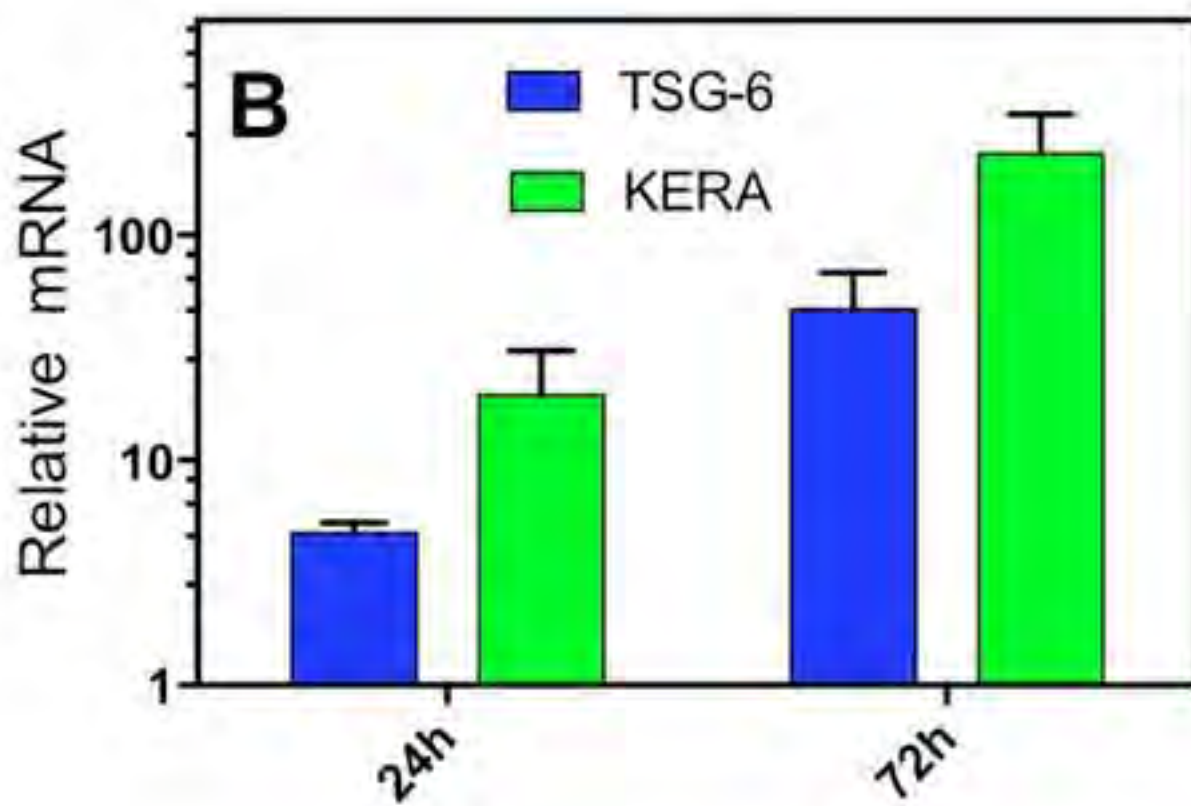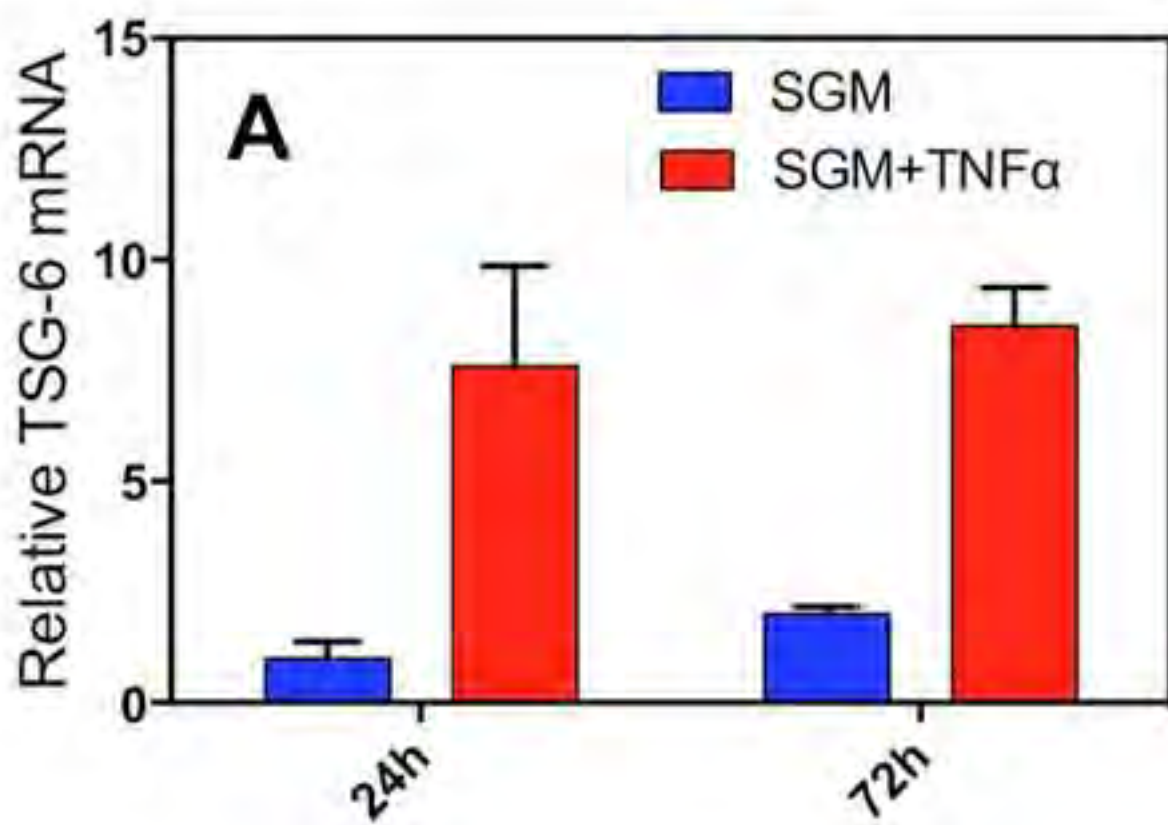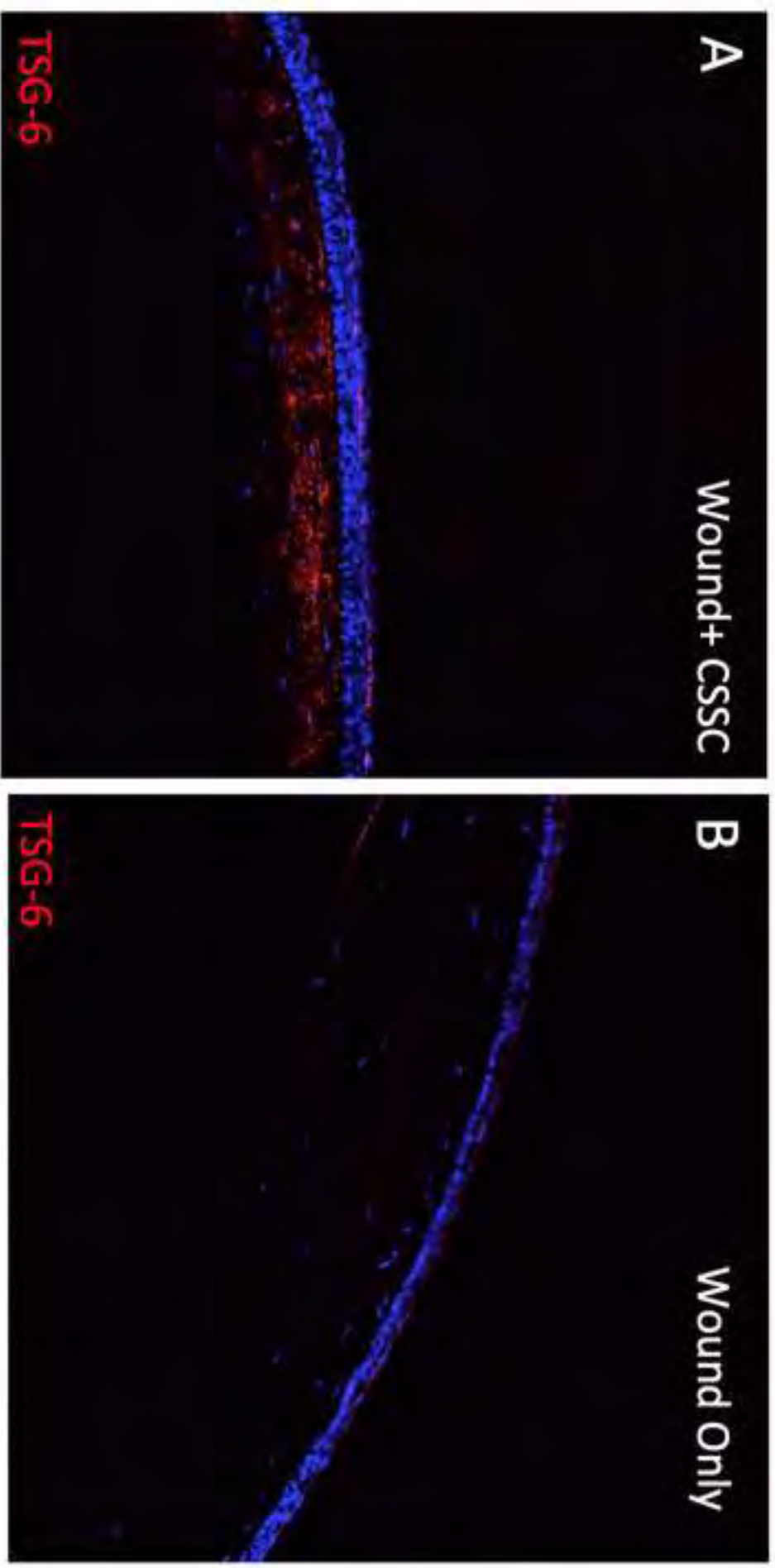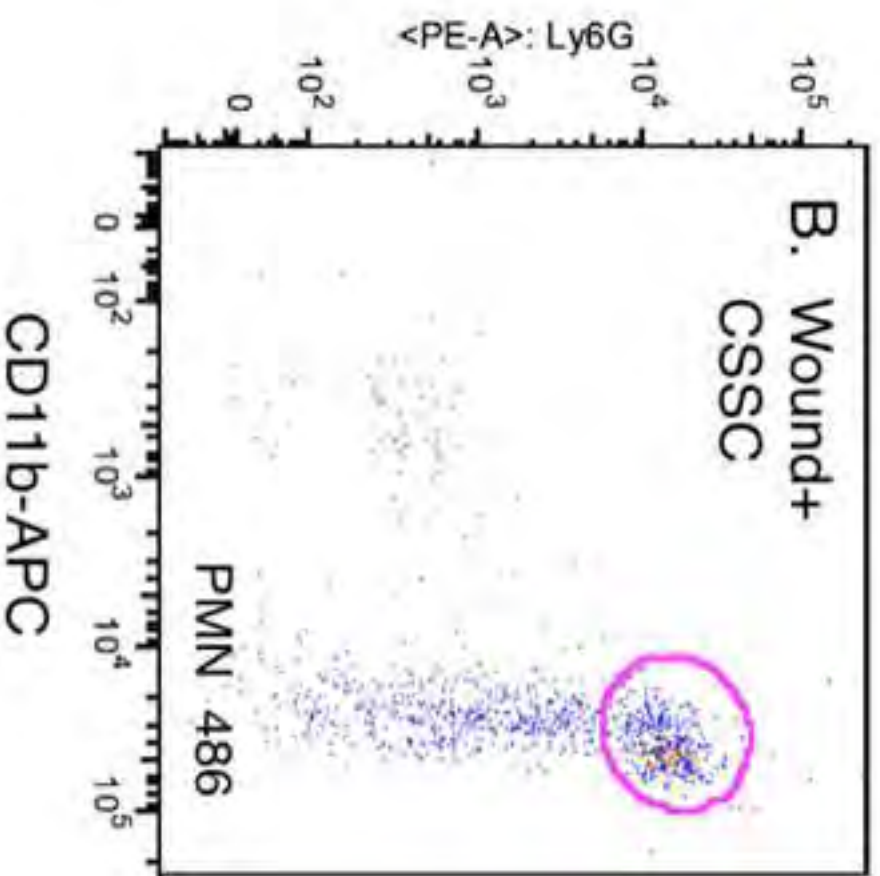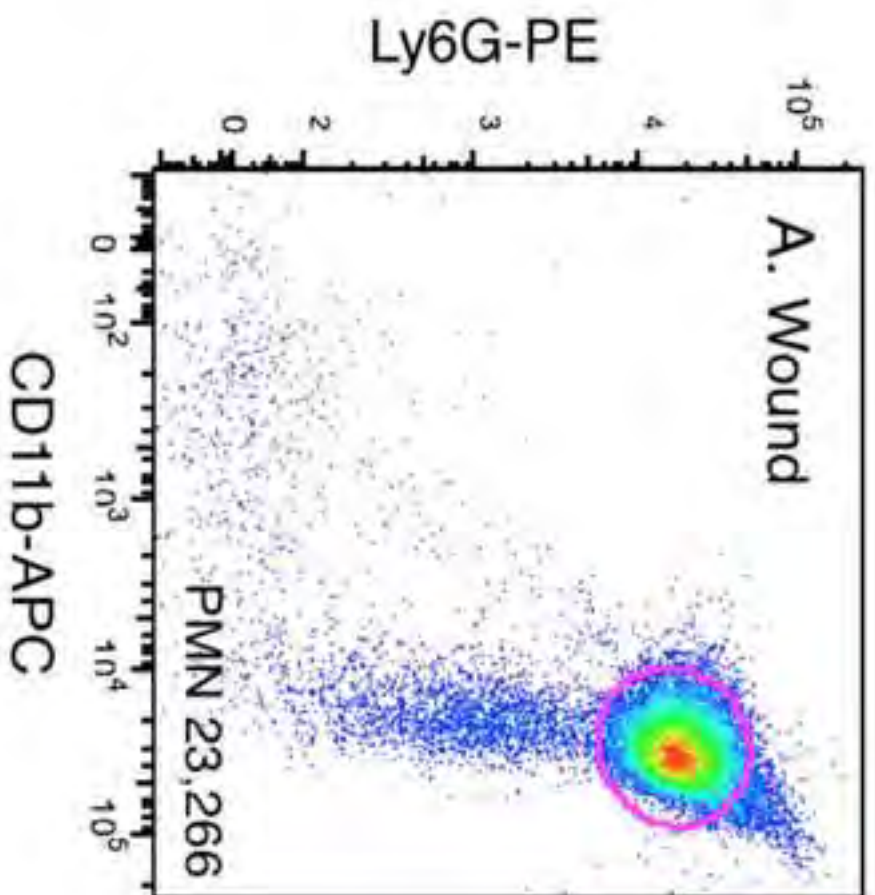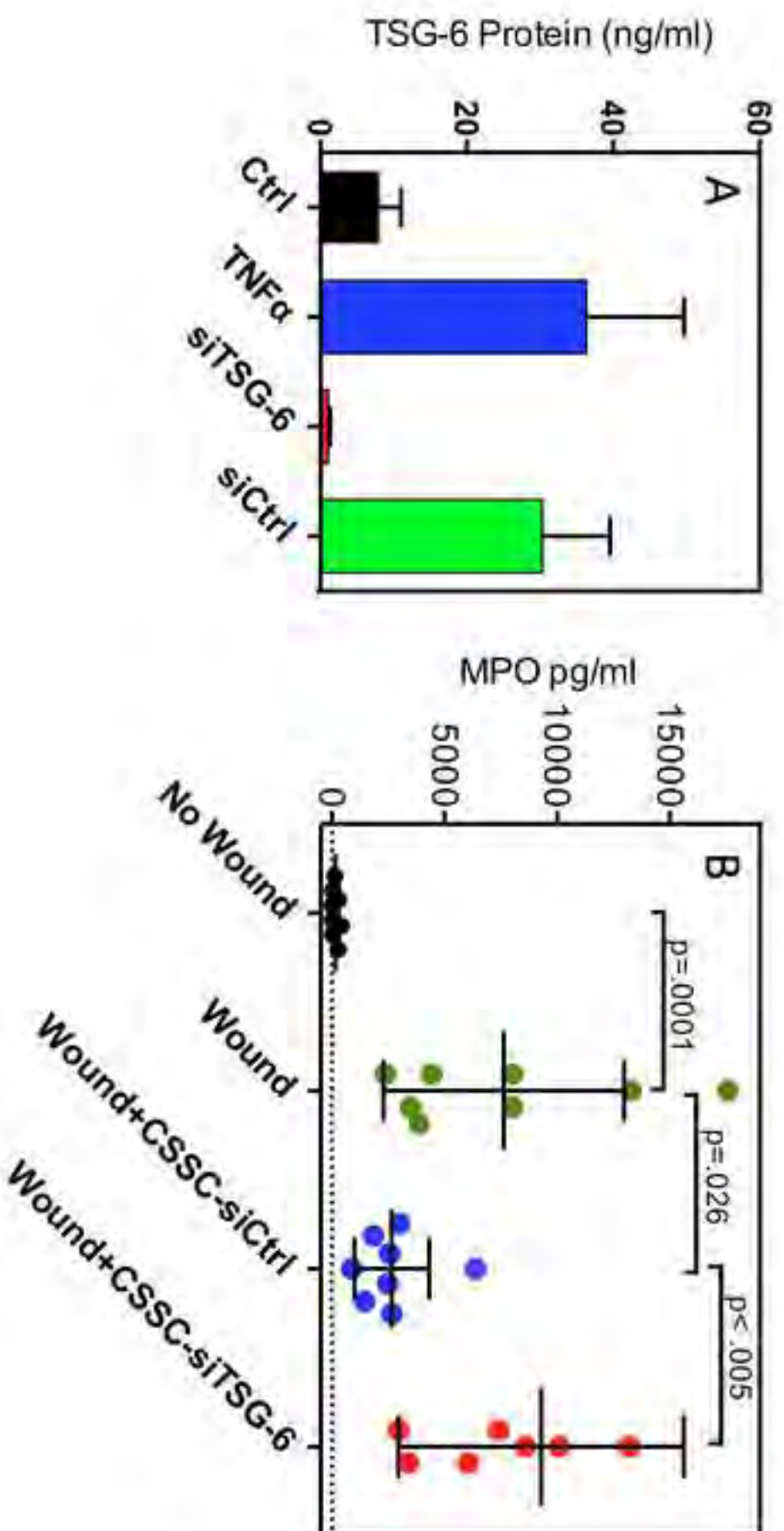
Controlling the Regenerative Potential of Corneal Stromal Stem Cells

View Session Detail   View Presentation

Add to Schedule   Print Abstract

Posterboard #: D0267

Abstract Number: 905 - D0267

Author Block: *Martha L. Funderburgh[1] , Golnar Shojaati[1,2] , Mary Mann[1] , Yiqin Du[1] , James L. Funderburgh[1]*

[1] Ophthalmology, Univ of Pittsburgh Sch of Med, Pittsburgh, Pennsylvania, United States; [2] Ophthalmology, University of Zurich, Zurich, Switzerland

Disclosure Block: Martha L. Funderburgh, None; Golnar Shojaati, None; Mary Mann, None; Yiqin Du, None; James L. Funderburgh, None

Purpose: Mesenchymal stem cells from human corneal stroma (CSSC) induce regeneration of transparent stromal tissue during wound repair in mice and are currently in process for usage in clinical trials for therapy of existing stromal scars. The mechanism by which corneal fibrosis is prevented, however, is not fully understood. In the absence of adhesive substratum, CSSC associate into spheroids. In an effort to understand factors controlling CSSC regenerative potential, this study compared properties of sphere-derived CSSC (Sp-CSSC) with substrate-attached CSSC (At-CSSC).

Methods: Limbal stromal tissue of donor corneal rims was dissected and collagenase digested, and CSSC were expanded at clonal density as described (PMID: 25504883). Spheres from passage 3-4 CSSC were formed in polyhema-coated dishes or in polypropylene tubes in DME/F12, B27, FGF2, and EGF at 10^5 cells/ml for 3 days, then dissociated with TrypLE to yield Sp-CSSC. Gene expression was examined by qPCR. Suppression of scarring was examined in a mouse model of corneal wound healing with 2×10^4 CSSC in a fibrin gel applied at the time of wounding. Neutrophil infiltration was assessed by ELISA for myeloperoxidase at 44 hr after wounding. Statistical significance was determined with t-test analysis of replicates using $p < 0.05$ as a criterion.

Results: Sp-CSSC had marked upregulation of genes associated with immunosuppressive activity including TSG-6, IL10, and COX2 compared to At-CSSC. TGFβ3, a cytokine associated with scarless wound healing, was upregulated > 100-fold as were CXCR4 and CXCL12, proteins involved in stem cell homing. In corneal wounds, Sp-CSSC completely suppressed neutrophil infiltration. At 14 days, expression of fibrotic markers (Fap, Tnc, Acta2,Tgfb1,Col3a1, Sparc) was significantly reduced in Sp-CSSC-treated wounds at levels similar to that of unwounded tissue. Suppression of fibrosis by Sp-CSSC was not statistically different from that of At-CSSC.

Conclusions: Sphere formation selects a CSSC population expressing high levels of genes associated with regenerative potential. In vivo, Sp-CSSC suppressed inflammation and prevented stromal fibrosis. These results suggest that sphere formation may help standardize the regenerative potential of cell lines from different donors, and may allow use of lower cell dosages in therapeutic applications.

Layman Abstract (optional): Provide a 50-200 word description of your work that non-scientists can understand. Describe the big picture and the implications of your findings, not the study itself

and the associated details.: We have recently discovered that stem cells can prevent or reverse scars in the cornea, a finding that may reduce the number of corneal transplants required to treat this blinding condition. Not all preprations of stem cells function similarly. This study developed a simple means of treating stem cells that may increase their potential to repair scars.

Corneal stromal tissue regeneration by stromal-derived stem cells

View Session Detail   View Presentation

Add to Schedule   Print Abstract

Abstract Number: 1853

Author Block: *James L. Funderburgh[1]*
[1] Univ of Pittsburgh School of Medicine, Pittsburgh, Pennsylvania, United States

Presentation Description: The limbal stroma contains a rare population of mesenchymal stem cells immediately subjacent to the epithelial basement membrane. These cells have been termed 'niche cells' because they exhibit direct contact with limbal epithelial stem cells and help maintain the LSC phenotype in vitro. The niche cells, when isolated and expanded in culture, exhibit properties of adult stem cells. Our work has shown these corneal stromal stem cells (CSSC) express genes typical of mesenchymal and embryonic stem cells as well as gene products present in neural crest cells and during ocular development. CSSC can be expanded $>10^7$ fold before senescence, providing an abundant resource for regenerative applications. When injected into the stroma of a lumican knockout mouse, human CSSC initiate tissue remodeling bringing matrix organization and transparency to the corneas. When CSSC are layered over a stromal debridement wound, fibrotic scar tissue is not deposited rather the ablated tissue is regenerated with matrix indistinguishable the original. This regenerative ability is accompanied by immune-suppressive properties of the CSSC. In vivo, neutrophil infiltration is suppressed after wounding and human CSSC do not elicit T-cell mediated rejection in mouse corneas. In vitro, CSSC block T-cell activation and proliferation. They also modify macrophage phenotype and expression of TGF betas, important mediators of fibrosis. These results implicate the regenerative properties of CSSC with their effect on the immune response of the host. Our current work focuses on the mechanism by which the CSSC exert these effects.